Phys. Lett. B 876 (2026) 140280

Contents lists available at ScienceDirect

Physics Letters B

journal homepage: www.elsevier.com/locate/physletb

Letter

Study of Higgs boson pair production in the $HH \rightarrow b\bar{b}\gamma\gamma$ final state with 308 fb^{-1} of data collected at $\sqrt{s} = 13$ TeV and 13.6 TeV by the ATLAS experiment

The ATLAS Collaboration[1]

ARTICLE INFO

Editor: Dr. M. Doser

Keywords:
ATLAS
Di-Higgs
Self-interaction
Photons
B-jets
Run 3

ABSTRACT

A search for Higgs boson pair production in the $b\bar{b}\gamma\gamma$ final state is performed. The proton–proton collision dataset corresponds to an integrated luminosity of 308 fb^{-1}, consisting of two samples, 140 fb^{-1} at a centre-of-mass energy of $\sqrt{s} = 13$ TeV and 168 fb^{-1} at $\sqrt{s} = 13.6$ TeV, recorded between 2015 and 2024 by the ATLAS detector at the CERN Large Hadron Collider. In addition to a larger dataset, this analysis improves upon the previous search in the same final state through several methodological and technical developments. The Higgs boson pair production cross section divided by the Standard Model prediction is found to be $\mu_{HH} = 0.9^{+1.4}_{-1.1}$ ($\mu_{HH} = 1^{+1.3}_{-1.0}$ expected), which translates into a 95% confidence-level upper limit of $\mu_{HH} < 3.7$. At the same confidence level the Higgs self-coupling modifier is constrained to be in the range $-1.6 < \kappa_\lambda < 6.6$ ($-1.8 < \kappa_\lambda < 6.9$ expected).

1. Introduction

Following the discovery of the Higgs boson (H) [1–6] by the ATLAS [7] and CMS [8] Collaborations, a central objective of the Large Hadron Collider (LHC) [9] programme is the exploration of the Higgs potential, which governs electroweak symmetry breaking (EWSB). In the Standard Model (SM) this potential is fully determined by the measured vacuum expectation value, $v \approx 246$ GeV, and the Higgs boson mass, $m_H \approx 125$ GeV. Deviations from the predicted form would indicate new physics with profound implications for particle physics and cosmology [10–13]. After EWSB, the Higgs potential is given by

$$V(H) = \frac{1}{2}m_H^2 H^2 + \lambda_3 v H^3 + \frac{1}{4}\lambda_4 H^4,$$

with $\lambda_3 = \lambda_4 = \lambda_{\mathrm{SM}} = \frac{m_H^2}{2v^2}$ in the SM. At the LHC it can be probed by studying the trilinear Higgs coupling which is accessible via Higgs boson pair (HH) production. The trilinear Higgs coupling is parameterised by a coupling modifier $\kappa_\lambda = \frac{\lambda_{3,\mathrm{meas}}}{\lambda_{\mathrm{SM}}}$, where $\lambda_{3,\mathrm{meas}}$ denotes its measured value. The quartic Higgs coupling, λ_4, for which the experimental sensitivity is very limited, has been marginally constrained so far by a search for triple Higgs boson production [14]. In gluon–gluon fusion (ggF), Higgs boson pairs are produced through diagrams involving either the trilinear Higgs vertex (Fig. 1(a)) or two top-quark Yukawa interaction vertices (Fig. 1(b)). Vector-boson fusion (VBF) production of Higgs boson pairs receives contributions from the trilinear Higgs vertex (Fig. 1(c)), VVH vertices (Fig. 1(d)), as well as the quartic $VVHH$ vertex (Fig. 1(e)), which exhibits sensitivity to non-SM contributions primarily at large values of the HH invariant mass. In both production modes the diagrams interfere destructively and the sensitivity to κ_λ lies mainly close to the HH production threshold. The production cross section depends in addition on the top-quark Yukawa coupling in the case of ggF, and on the VVH (κ_V) and $VVHH$ (κ_{2V}) coupling modifiers for VBF.

The predicted cross sections in the SM are very small, namely $\sigma^{HH}_{\mathrm{ggF}} = 30.8^{+2.0}_{-7.1}$ fb [15–24] and $\sigma^{HH}_{\mathrm{VBF}} = 1.69 \pm 0.05$ fb [25–28] for proton–proton (pp) collisions at a centre-of-mass energy of $\sqrt{s} = 13$ TeV,[1] about three orders of magnitude smaller than for single Higgs boson production. At 13.6 TeV they rise to $34.1^{+2.2}_{-7.9}$ fb and 1.87 ± 0.05 fb, respectively [15–28].

This Letter reports on an updated analysis of HH production in the $HH \rightarrow b\bar{b}\gamma\gamma$ channel. Although this channel represents only 0.26% of the HH events, it benefits from the excellent di-photon mass resolution and offers the highest efficiency among the leading search channels near the HH production threshold, where the sensitivity to κ_λ is the greatest. The analysis uses the full LHC Run-2 pp collision dataset of 140 fb^{-1} at $\sqrt{s} = 13$ TeV collected by the ATLAS experiment and a portion of the Run-3 dataset (2022–2024) corresponding to 168 fb^{-1} at

---

[1] The cross section prediction changed slightly compared to the one used in the previous iteration of this analysis as detailed in Ref. [29] due to a new set of parton distribution functions and the inclusion of electroweak corrections for VBF.

Contact authors: ATLAS Publications (atlas.publications@cern.ch).

[1] See Appendix for the list of collaboration members.

https://doi.org/10.1016/j.physletb.2026.140280
Received 8 July 2025; Received in revised form 12 February 2026; Accepted 13 February 2026
Available online 23 February 2026

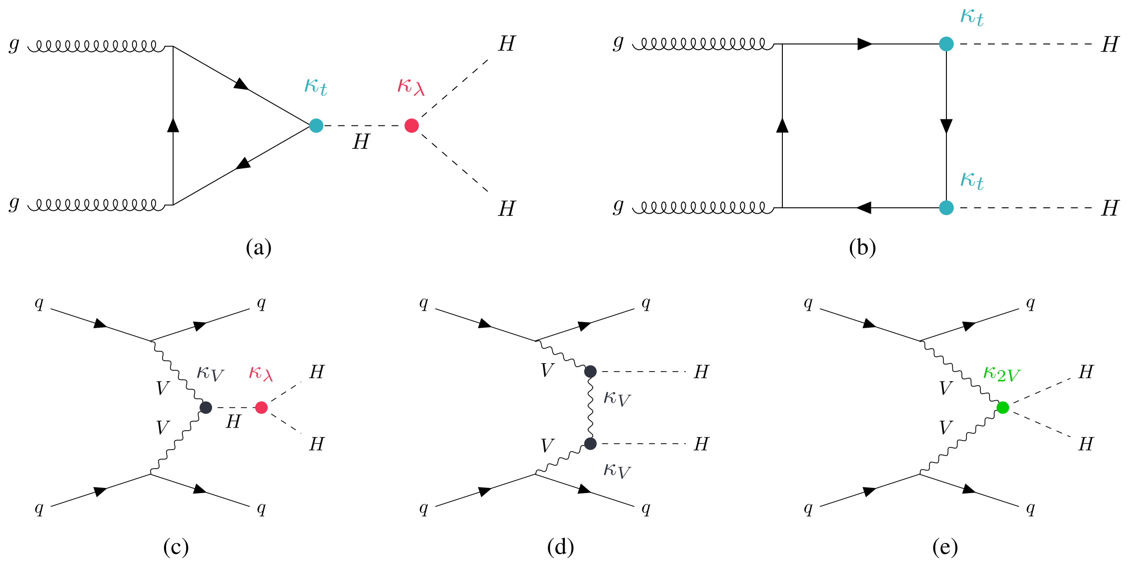

Fig. 1. Leading-order Feynman diagrams for (a,b) the dominant ggF production and (c-e) VBF production of Higgs boson pairs, where (a,c) involve the trilinear Higgs coupling, (b,d) have two independent single Higgs vertices and (e) contains the $VVHH$ vertex. The coupling modifiers for the ttH, VVH and $VVHH$ couplings are represented by κ_t, κ_V, κ_{2V}, respectively.

$\sqrt{s} = 13.6$ TeV. After pre-selection, events are categorised according to the $b\bar{b}\gamma\gamma$ invariant mass, signal purity, and data-taking period. A fit to the di-photon mass distribution is then performed across categories, with the background modelled using analytic functions. The analysis is improved in several aspects compared to the previous iteration [29]. The most significant are a new b-tagging algorithm based on transformer neural networks (GN2) [30–33] and a kinematic fit to improve the $b\bar{b}$ and $b\bar{b}\gamma\gamma$ invariant mass resolutions.

During LHC Run 2, an extensive programme was carried out by ATLAS and CMS to search for HH production and constrain κ_λ in the $b\bar{b}\gamma\gamma$ channel [29,34], as in several other final states [35–44]. Combining all channels, ATLAS and CMS constrained at 95% confidence level (CL) the HH signal strength μ_{HH}, defined as the observed Higgs boson pair production cross section divided by the SM prediction, to be $\mu_{HH} < 2.9$ [45] and $\mu_{HH} < 3.4$ [46] respectively, assuming the SM HH kinematics. The trilinear Higgs coupling modifier was constrained at the same confidence level by ATLAS to be $-1.2 < \kappa_\lambda < 7.2$ [45] and by CMS to be $-1.4 < \kappa_\lambda < 7.8$ [47].

2. ATLAS detector

The ATLAS experiment [48,49] at the LHC is a multipurpose particle detector with a forward–backward symmetric cylindrical geometry and a near 4π coverage in solid angle.[2] It consists of an inner tracking detector surrounded by a thin superconducting solenoid providing a 2 T axial magnetic field, electromagnetic and hadronic calorimeters, and a muon spectrometer. The inner tracking detector covers the pseudorapidity range $|\eta| < 2.5$. It consists of silicon pixel, silicon microstrip, and transition radiation tracking detectors. Lead/liquid-argon (LAr) sampling calorimeters provide electromagnetic (EM) energy measurements with high granularity within the region $|\eta| < 3.2$. A steel/scintillator-tile hadronic calorimeter covers the central pseudorapidity range ($|\eta| < 1.7$). The endcap and forward regions are instrumented with LAr calorimeters for EM and hadronic energy measurements up to $|\eta| = 4.9$. The muon spectrometer surrounds the calorimeters and is based on three large superconducting air-core toroidal magnets with eight coils each. The field integral of the toroids ranges between 2.0 and 6.0 Tm across most of the detector. The muon spectrometer includes a system of precision tracking chambers up to $|\eta| = 2.7$ and fast detectors for triggering up to $|\eta| = 2.4$. The luminosity is measured mainly by the LUCID–2 detector which is located close to the beampipe. A two-level trigger system was used to select events [50,51]. The first-level trigger is implemented in hardware and it uses a subset of the detector information to accept events at a rate close to 100 kHz. This is followed by a software-based trigger that reduced the accepted rate of complete events to 1.25 kHz and 3 kHz on average in Run 2 and Run 3, respectively, depending on the data-taking conditions. A software suite [52] is used in data simulation, in the reconstruction and analysis of real and simulated data, in detector operations, and in the trigger and data acquisition systems of the experiment.

3. Data and simulation samples

The analysis presented in this Letter uses pp-collision data collected by the ATLAS experiment during the LHC Run 2 at $\sqrt{s} = 13$ TeV (from 2015 to 2018) and during the first part of the LHC Run 3 at $\sqrt{s} = 13.6$ TeV (from 2022 to 2024). Data quality requirements for Run 2 and Run 3 are detailed in Ref. [53]. The resulting integrated luminosity is $140.1 \pm 1.2\ \text{fb}^{-1}$ for the Run-2 dataset [54] and $168.0 \pm 6.7\ \text{fb}^{-1}$ for the Run-3 dataset,[3] respectively.

This analysis searches for Higgs boson pair production in the $b\bar{b}\gamma\gamma$ final state, considering as signal both the dominant ggF and the subdominant VBF production modes. For the Monte Carlo (MC) simulation of the ggF signal, events are generated using POWHEG BOX v2 [55–59] with parton distribution functions (PDFs) from the PDF4LHC21 [60]

---

[2] ATLAS uses a right-handed coordinate system with its origin at the nominal interaction point (IP) in the centre of the detector and the z-axis along the beam pipe. The x-axis points from the IP to the centre of the LHC ring, and the y-axis points upwards. Polar coordinates (r, ϕ) are used in the transverse plane, ϕ being the azimuthal angle around the z-axis. The pseudorapidity is defined in terms of the polar angle θ as $\eta = -\ln\tan(\theta/2)$ and is equal to the rapidity $y = \frac{1}{2}\ln\left(\frac{E+p_z}{E-p_z}\right)$ in the relativistic limit. Angular distance is measured in units of $\Delta R \equiv \sqrt{(\Delta y)^2 + (\Delta\phi)^2}$.

[3] The preliminary luminosity for the 2024 data was estimated by using the number of $Z \to ee$ and $Z \to \mu\mu$ events relative to those in the 2022/2023 data within a preliminary uncertainty of 5%. Combined with the 2% uncertainty for 2022/2023 [111], this results in a luminosity-weighted uncertainty for the Run-3 dataset of 4%.

set. In addition to the SM sample, where the value of κ_λ is set to 1, other samples corresponding to beyond-the-SM (BSM) scenarios are generated with $\kappa_\lambda = -1$, 0, 2.5, 5 and 10, respectively. For VBF HH signal events, MadGraph5_aMC@NLO [61] is used in the leading-order (LO) generation with the five-flavour scheme and the NNPDF3.0NLO [62] PDF. Furthermore, 12 additional VBF HH samples are generated with the same settings as the nominal sample, but using BSM combinations of the coupling modifiers κ_λ, κ_{2V} and κ_V. In both cases, PYTHIA 8.309 [63] is used for the simulation of the Higgs boson decays, parton showering, hadronisation and underlying event with the A14 set of tune parameters [64]. In the generation of the Higgs boson decay into photons [55–57,65–71], Dalitz events (*i.e.* the decay in which one of the two photons is off-shell) are not included. The decays of bottom and charm hadrons are simulated using the EVTGEN 1.6.0 programme [72].

In this search, di-photon background processes are of two types: resonant production of a single Higgs boson decaying into $\gamma\gamma$ and continuum non-resonant di-photon production in association with jets. Background from inclusive production of events with either one photon and one jet (γj) or two jets (jj), where one or two jets mimic the signature of one or two photons, respectively, is taken into account using a data-driven approach. All the main single Higgs boson production modes are generated, mostly following the same procedure as in Ref. [29], including ggF, VBF, production in association with a W or Z boson, with a $t\bar{t}$ or $b\bar{b}$ pair, or with a single top-quark. Dalitz decays of the Higgs boson are not included here either. Continuum di-photon production in association with jets from quarks of any flavour ($\gamma\gamma$ + jets) is also simulated. An additional sample of simulated continuum di-photon plus two b-jets events ($\gamma\gamma + b\bar{b}$) is generated and used for the study of the background di-photon invariant mass distribution, as described in Section 5. For the simulation of continuum di-photon events, SHERPA 2.2.14 [73] is used for both the event generation and the parton showering, and the NNPDF3.0NNLO PDF set is adopted.

All simulated signal and background events are passed through a detailed simulation of the ATLAS detector [74] based on GEANT4 [75], except BSM signal samples (*i.e.* where the value of at least one of the coupling modifiers κ_λ, κ_{2V} or κ_V is not set to 1) and the non-resonant di-photon samples ($\gamma\gamma$ + jets and $\gamma\gamma + b\bar{b}$), which are interfaced to a fast detector simulation based on a parametric description of the calorimeter showers [76]. The difference between the results obtained with full simulation and with fast simulation is within the statistical uncertainty, when considering the upper limits on μ_{HH} and the κ_λ constraints. The Higgs boson mass is assumed to be 125 GeV, a value consistent with the latest measurements [77], in all simulations. Additional inelastic pp collisions occurring in the same or nearby bunch crossings, referred to as *pileup*, are also simulated and matched to the distribution observed in data, as described in Refs. [29,78].

4. Object and event selections

The results were obtained using the software framework documented in Ref. [79], developed for collision data analysis within the ATLAS Collaboration. The analysis flow begins with the selection of events containing exactly two well-reconstructed photons and at least two b-jet candidates [30]. This pre-selection, briefly summarised in Section 4.1, reduces the background while maintaining good signal acceptance times efficiency. The selected events are then classified into mutually exclusive categories based on the invariant mass of the $b\bar{b}\gamma\gamma$ system and multivariate discriminants. The event categorisation, described in Section 4.2, is designed to optimise sensitivity to the $HH \rightarrow b\bar{b}\gamma\gamma$ process and to the coupling modifiers κ_λ and κ_{2V}.

4.1. Event pre-selection

To identify $H \rightarrow \gamma\gamma$ decays, events were collected with di-photon triggers with nominal transverse momentum (p_{T}) thresholds of 35 GeV and 25 GeV for the leading and sub-leading photon, respectively, and satisfying online photon identification requirements [51,80]. In Run 3, from 2023 onwards, with the upgrade of the first-level trigger system, more granular information from EM calorimeters is used, which results in similar performance compared to Run 2, in an environment with a higher level of pileup [51]. Of all reconstructed collision vertices, the primary vertex (PV) is selected as the one with the highest sum of squared transverse momenta of contributing tracks $\sum p_{\mathrm{T}}^2$ [81]. Selecting the correct PV ensures that all reconstructed objects are associated with the hard-scatter collision and improves the $\gamma\gamma$ mass resolution.

Selected events are required to contain two photon candidates in the acceptance of the finely segmented part of the EM calorimeter ($|\eta| < 1.37$ or $1.52 < |\eta| < 2.37$). Photons are reconstructed from EM calorimeter signals exceeding noise thresholds using dynamic topological clustering, with additional clusters included for photon conversion products when applicable [82]. The photon candidates are calibrated [83] and identified by an algorithm that relies on the shape of the EM showers reconstructed in the calorimeter [84]. A *loose* working point, corresponding to high signal efficiency at the cost of reduced background rejection, is used to match to the photon candidates selected by the trigger. The final selection of photon candidates is made using a *tight* selection, which provides high background rejection at the cost of reduced signal efficiency. Photon candidates must also satisfy isolation requirements based on the energy flow in the calorimeter and the total transverse momentum of charged-particle tracks from the PV, measured in cones surrounding the photon direction [82]. The two leading photons satisfying these selections are required to have an invariant mass $m_{\gamma\gamma}$ between 105 and 160 GeV and transverse momenta above 35% and 25% of $m_{\gamma\gamma}$, respectively. The $m_{\gamma\gamma}$ *sidebands* are defined as data entries within the mass window of $m_{\gamma\gamma} \in [105, 160]$ GeV, excluding the signal region from 120 to 130 GeV.

Jets are reconstructed from particle-flow objects built from noise-suppressed positive-energy topological clusters in the calorimeter and reconstructed tracks using the anti-k_t clustering algorithm with the radius parameter $R = 0.4$ [85,86]. Jet candidates are required to have $p_{\mathrm{T}} > 25$ GeV and $|y| < 4.5$. Jets contained in the fiducial acceptance of the inner detector ($|\eta| < 2.4$) and with $p_{\mathrm{T}} < 60$ GeV must be identified by a 'jet-vertex tagger' as originating from the PV [87], while those outside of this region must be identified by a 'forward jet-vertex tagger' [88]. To target $H \rightarrow b\bar{b}$ decays, events are required to contain at least two b-tagged jets, which are *central* jets (those in the acceptance of the inner detector $|\eta| < 2.5$) that satisfy the criteria of the GN2 b-tagging classification algorithm with an efficiency of 85% for b-jets and a misidentification rate of 0.01 (0.20) for light-flavour (charm) jets in simulated $t\bar{t}$ events [30–33]. These loose requirements are chosen to maximise the signal acceptance and correspond to the optimal analysis sensitivity. If there are more than two b-tagged jets in an event, the jets with the highest b-tagging scores (*i.e.* the output discriminant of the GN2 algorithm) are selected to form the $H \rightarrow b\bar{b}$ candidate. The b-tagging score distribution is discrete, so that each bin corresponds to a given b-tagging efficiency range. If two or more jets are in the same bin of the b-tagging score distribution, those with the highest transverse momenta are selected as $H \rightarrow b\bar{b}$ candidate jets. Two corrections are applied to the energy of the b-tagged jets to account for possible contributions from muons originating from semileptonic b-hadron decays (Muon-in-jet correction) and undetected energy from neutrinos and out-of-cone effects (PtReco correction) [29]. These corrections improve the resolution of the invariant mass of the two b-jet candidates from the $H \rightarrow b\bar{b}$ decay ($m_{b\bar{b}}$) by up to 17%.

Similarly to Ref. [89], a kinematic fit (KF) is performed to improve the resolution of $m_{b\bar{b}}$ and the invariant mass of the system with two photons and two b-jets ($m_{b\bar{b}\gamma\gamma}$), in a two-step process. In the first step, the KF exploits momentum conservation in the transverse plane to correct jet energies and momenta using the di-photon kinematics. In the second step, an additional term is introduced to further enhance the resolution with which $m_{b\bar{b}\gamma\gamma}$ is reconstructed by constraining $m_{b\bar{b}}$ to the

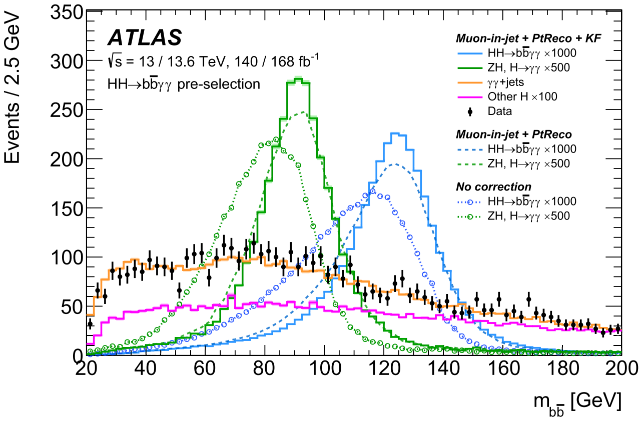

Fig. 2. Di-jet invariant mass distribution of b-tagged jets ($m_{b\bar{b}}$) after the analysis pre-selection, shown for data as well as for simulated $HH \to b\bar{b}\gamma\gamma$ signal, ZH ($H \to \gamma\gamma$), $\gamma\gamma$ +jets, and other single Higgs boson backgrounds (denoted by 'other H'). Also shown are the $HH \to b\bar{b}\gamma\gamma$ and ZH ($H \to \gamma\gamma$) distributions after applying the Muon-in-jet, PtReco, and the first-step kinematic fit (KF) corrections. The shaded regions on the histograms indicate the size of the statistical uncertainties. All simulated distributions are scaled by the factors shown in the legend, except for $\gamma\gamma$ +jets, which is normalised to the sidebands of the $m_{\gamma\gamma}$ distribution in data.

Higgs boson mass through a quadratic term, $(m_{b\bar{b}} - 125\,\text{GeV})^2$, added to the log-likelihood function being minimised to balance the HH system. Independent detector-response functions of the jet energies and transverse momenta are computed using simulated HH events. The probability density functions of the x and y components of the total transverse momentum of the di-photon system and all jets in the event, as derived from simulation, are used in the KF. The fit output is a correction factor α applied to both the energy and the p_{T} of the jet. The α factor is evaluated for each jet in the event. The photon momenta are not corrected by the KF given the excellent detector resolution and to avoid biasing the $m_{\gamma\gamma}$ distribution. The corrected jet momenta from the second step are used through the rest of the analysis while, in the multivariate event discrimination, the $m_{b\bar{b}}$ value from the first step of the KF is used to avoid distortions of the background. After the second KF step, the resolution on $m_{b\bar{b}\gamma\gamma}$ is improved by 46%. Fig. 2 shows the $m_{b\bar{b}}$ distribution for data and for simulated signal and background processes. The HH and ZH simulated events are shown both before and after applying the Muon-in-jet and PtReco corrections, as well as after the first-step KF. The suite of corrections and the KF improve the $m_{b\bar{b}}$ resolution by up to 27%.

Events with six or more central jet candidates, or with one or more isolated lepton (electron or muon) candidates with $p_{\text{T}} > 10\,\text{GeV}$ and satisfying the lepton *medium* identification criteria [84,90] are rejected to suppress the background from $t\bar{t}H(\gamma\gamma)$ and inclusive $t\bar{t}$ production. No requirement is made on the number of *non-central* jets (those beyond the acceptance of the inner detector $|\eta| \geq 2.5$).

The efficiency of the event pre-selection is 17% and 11% for SM ggF HH and SM VBF HH events, respectively, with the largest losses arising from the di-photon acceptance and b-jet requirements. The requirement of having at least two b-jets is less efficient for the VBF HH events (35%) than for the ggF HH events (49%). A total of 2 795 and 3 321 events are pre-selected in the Run-2 and Run-3 data, respectively. According to the SM prediction, a total of about five HH events are expected after the analysis pre-selection. In this data sample, approximately 74% of the continuum background events contain two prompt photons, 24% contain one prompt photon and one misidentified jet, and 2% contain two misidentified jets, as determined with data-driven techniques [91]. The fractions of these components in Run 2 and Run 3 are consistent within the statistical uncertainties. Fig. 3 shows the $m_{\gamma\gamma}$ distributions of data and simulated events after pre-selection for Run 2 and Run 3.

4.2. *Event categories*

Anomalous values of the coupling modifiers κ_λ and κ_{2V} not only affect the HH signal production cross section but also modify the kinematic properties of the HH system. For example, κ_λ values different from unity mostly result in a softer HH invariant mass spectrum [92], while anomalous values of κ_{2V} tend to harden the spectrum. The events are therefore classified in two regions based on the improved four-body invariant mass $m^*_{b\bar{b}\gamma\gamma} = m_{b\bar{b}\gamma\gamma} - (m_{b\bar{b}} - 125\,\text{GeV}) - (m_{\gamma\gamma} - 125\,\text{GeV})$: a *high-mass* region and a *low-mass* region are defined by setting a 350 GeV boundary on $m^*_{b\bar{b}\gamma\gamma}$. The use of $m^*_{b\bar{b}\gamma\gamma}$ over $m_{b\bar{b}\gamma\gamma}$ improves the signal mass resolution by up to 10% due to the cancellation of detector resolution effects [93]. In each of the two $m^*_{b\bar{b}\gamma\gamma}$ regions, a dedicated boosted-decision-tree (BDT) discriminant is trained to distinguish HH signals from the background arising from $H \to \gamma\gamma$ decays in single Higgs boson production and from the continuum $\gamma\gamma$ +jets events. The training is performed with the XGBoost programme [94] using simulated Run-2 and Run-3 collision events combined according to the SM expectations. As explained below, Run-2 and Run-3 data events are classified separately. In the high-mass region, the signal samples used for training include a mixture of SM ggF and VBF HH events, as well as five BSM samples of VBF HH events with $(\kappa_\lambda, \kappa_{2V}, \kappa_V)$: (0, 1, 1), (10, 1, 1), (1, 1.5, 1), (1, 3, 1), and (−5, 1, 0.5). The BSM VBF HH samples are used for the training in the high-mass region to increase the sensitivity to κ_{2V}. In the low-mass region, the signal samples consist of BSM ggF HH events corresponding to $\kappa_\lambda = 10$ and $\kappa_\lambda = 5$, plus the five BSM VBF HH samples already used in the high-mass region. The mixture of BSM samples used for the training in both the high-mass and low-mass regions cover a wide range of anomalous values of κ_λ and κ_{2V}. Variations of the order of unity on the κ_λ value used in the training samples have a negligible impact on the final results. In both regions, the background samples used for the training include single Higgs boson production and continuum di-photon production in association with jets. The relative weights assigned to each input sample in the mixture of the training dataset, as well as the values of the XGBoost hyperparameters, were tuned in Ref. [29] and their values were found to be optimal for this analysis. The BDT discriminants use the same input variables as in Ref. [29]. They include kinematic properties of the two photon and two b-jet candidates, as well as event-level kinematic quantities such as $m^*_{b\bar{b}\gamma\gamma}$. The input variables are chosen in order to avoid distortions of the $m_{\gamma\gamma}$ distribution, which is used as the analysis observable in the final fit to the data, after placing a selection requirement on the BDT output score. In particular, the p_{T} of each of the two photons normalised to $m_{\gamma\gamma}$ are included in the input. Additional variables include, for events with more than two jets, the p_{T}, η, ϕ, and discrete b-tagging scores of the third and fourth jets. Events with at least four jets can arise from VBF HH production, in which the two final-state jets have high transverse momenta and are separated by a large rapidity gap. VBF jet candidates are selected as those belonging to the pair with the largest invariant mass among all possible pairs in the event excluding the $H \to b\bar{b}$ jet candidates. Their invariant mass and pseudorapidity difference are then used as additional input variables in the BDTs. In simulated SM VBF HH events with at least four jets, the correct VBF jet pair is identified in 88% of events.

The two BDT scores are used to define output categories with different signal purities. They are designed to maximise the overall number-counting significance [95] for a benchmark signal using HH and background yields in the di-photon invariant mass range $120\,\text{GeV} < m_{\gamma\gamma} < 130\,\text{GeV}$. In the high-mass region, the signal yield is computed from the sum of the expected SM ggF and VBF HH contributions, while in the low-mass region, the benchmark signal is defined using a mixture of two ggF and VBF HH samples with large values of κ_λ in order to cover a wide range of BSM scenarios. During this optimisation process, each category is required to contain at least eleven expected continuum background events from the region $105\,\text{GeV} < m_{\gamma\gamma} < 160\,\text{GeV}$ in the

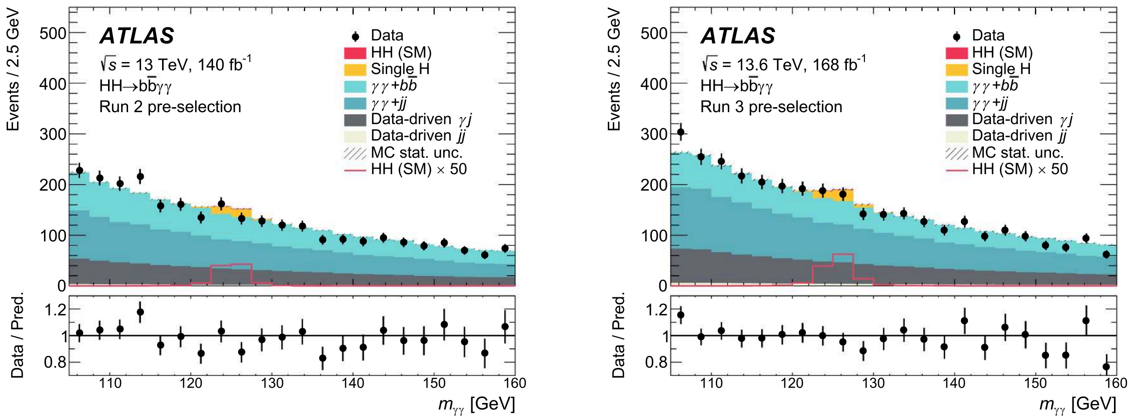

(a) (b)

Fig. 3. Distributions of the di-photon invariant mass for events in data compared with the sum of the expected signal and background contributions after pre-selection for (a) Run 2 and (b) Run 3. The relative fractions of the simulated $\gamma\gamma + b\bar{b}$ and $\gamma\gamma + jj$ (where j is a light-flavour or gluon jet) events are determined from the generator-level flavour decompositions of the inclusive $\gamma\gamma$ +jets sample. The various continuum background components are then normalised using a data-driven photon purity measurement [91] such that their sum is consistent with the data in the sidebands. The HH signal is shown as a filled histogram stacked on top of the backgrounds, normalised to the SM prediction. It is also shown unstacked as an unfilled histogram, scaled by the factor indicated in the legend to enhance visibility.

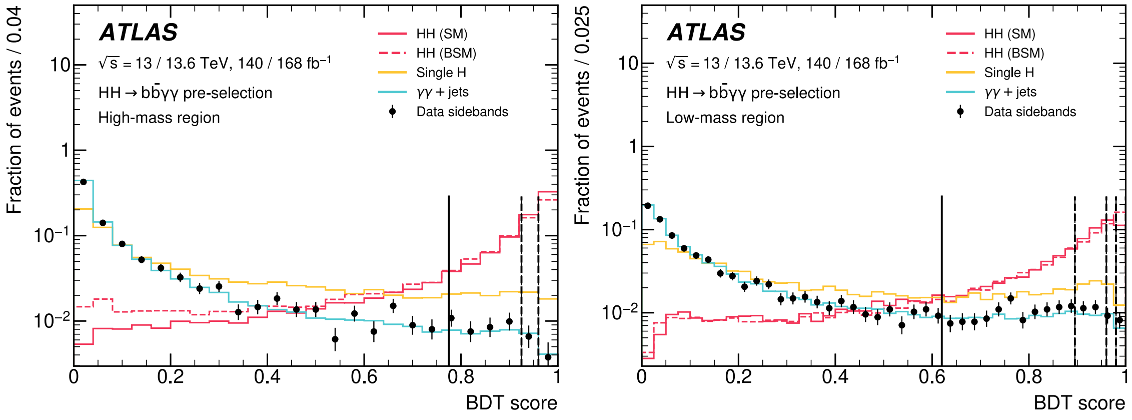

(a) (b)

Fig. 4. BDT score distributions using combined Run-2 and Run-3 samples for ggF HH and VBF HH signal events and the two main background components ($\gamma\gamma$ + jets continuum background and single Higgs boson processes) for the (a) high-mass and (b) low-mass regions. Data sideband events are also shown. Simulated events are contained in the interval $m_{\gamma\gamma} \in [105, 160]$ GeV. All distributions are normalised to unity. The vertical dashed lines correspond to the thresholds used to define the event categories. Events with a BDT score below the lowest threshold (solid line) are discarded.

combined samples of Run-2 and Run-3 simulated events. Under the assumption of a Poisson distribution, eleven simulated events in this combined sample correspond to a data sample expected to contain at least two events. This ensures a sufficient number of events for constraining the shape of the di-photon invariant mass distribution of the continuum background when performing the fit to the data. This approach allows a more stringent selection requirement on the BDT score, resulting in a 10% improvement in signal significance compared to a strategy with separated trainings for Run 2 and Run 3, and for which the requirements on continuum background simulated events are applied to the corresponding BDTs individually.

After the optimisation, three categories (labelled 'High Mass i', i = 1..3) in the high-mass region and four categories (labelled 'Low Mass i', i = 1..4) in the low-mass region are defined based on the corresponding BDT scores, with a higher category index i corresponding to higher BDT scores and more signal-like events. The addition of further categories did not improve the results significantly. Events with a BDT score lower than the threshold defining the category with the lowest index (*i.e.* the category with the lowest signal sensitivity) are discarded. Data events from the inclusive signal region are thus classified in fourteen (two sets of seven) exclusive signal regions based on the value of $m^*_{b\bar{b}\gamma\gamma}$, the corresponding BDT scores and the data-taking period (*i.e.* Run 2 or Run 3).

The BDT discriminant distributions in the high- and low-mass regions observed in data in the $m_{\gamma\gamma}$ sidebands for Run 2 and Run 3 combined are shown in Fig. 4. The BDT score distributions for the dominant non-resonant background from the $\gamma\gamma$ + jets sample, the resonant single Higgs boson background, and the combined ggF and VBF HH signals for different values of κ_λ and κ_{2V}, all taken from simulation, are also shown. The BDT categories are indicated by vertical dashed lines. In total, 293 and 342 events are retained in the Run-2 and Run-3 datasets, respectively. Among these, 239 Run-2 and 269 Run-3 events lie in the $m_{\gamma\gamma}$ sidebands.

5. Signal and background modelling

For the extraction of the statistical results, a simultaneous fit is performed to all data in the fourteen event categories. The signal and non-resonant background yields in each event category are determined from the combined unbinned fit to the di-photon invariant mass distributions, while the resonant background yields are fixed to the SM expectation. The signal yields for ggF and VBF HH production are parameterised as a function of the relevant coupling modifiers by performing a linear combination of the relevant simulation samples. The differential VBF HH cross section can be written as a polynomial of the coupling modifiers, whose coefficients are determined using six reference samples for $(\kappa_\lambda, \kappa_{2V}, \kappa_V)$: (1, 1, 1), (1, 1, 0.5), (10, 1, 1), (1, 1.5, 1), (2, 1, 1), and (−5, 1, 0.5). Similarly, the ggF HH cross section is expressed as a function of κ_λ using three samples with $\kappa_\lambda = 0, 1, 5$.

The signal and background $m_{\gamma\gamma}$ distributions in each category are independently modelled with analytical functions. For signal and resonant background events, double-sided Crystal Ball functions [96–98] are used. The nominal shape parameters are obtained from fits to simulated SM HH events, with ggF and VBF modes weighted according to their SM cross sections and summed. In the final fit to data, the Gaussian core parameters, describing the peak and width of the distribution, are allowed to float within the uncertainties arising from the photon energy calibration, while the tail parameters are fixed to their nominal values.

Signal shapes are parameterised for Run 2 and Run 3 separately. The same model is found to describe well single Higgs boson and Higgs boson pair simulated events for both SM and non-SM coupling modifier values.

The $m_{\gamma\gamma}$ distributions of the non-resonant di-photon background are modelled with exponential functions, whose normalisation and shape parameters are obtained from the fit to the data. The chosen exponential function in each category is found to describe well the data in the $m_{\gamma\gamma}$ sidebands, as well as the background-only template obtained with a sample of simulated $\gamma\gamma + b\bar{b}$ events normalised to the data in the $m_{\gamma\gamma}$ sidebands. The background shape parameters are correlated for each Run-2 and Run-3 category pair (*e.g.* High Mass 1 for Run 2 and High Mass 1 for Run 3) in the fit to the data, ensuring consistency with the requirement on the minimum expected number of continuum background events to define category boundaries, as described in Section 4. Tests using the large sample of simulated $\gamma\gamma + b\bar{b}$ continuum background events, as well as from a comparison of data-sideband distributions in the low-mass and high-mass regions, indicate good compatibility between the Run-2 and Run-3 shape parameters at the current level of precision of this analysis. Furthermore, no significant bias on the fitted signal is observed even when enhancing the difference between Run-2 and Run-3 background shapes by a factor of ten compared to those seen in simulation. Finally, the impact of correlating or decorrelating the parameters of the analytical model describing the shape of the background is found to be negligible. Normalisation parameters of the background functions are not correlated.

6. Systematic uncertainties

Systematic uncertainties affect the di-photon invariant mass distribution of both the HH signal and single Higgs boson background. However, their impact remains relatively minor compared with the statistical uncertainty, which dominates due to the limited number of data events and the use of data-driven methods for modelling the dominant continuum background.

The *spurious signal* is defined as the maximum absolute value of the bias on the fitted signal yield. To estimate it, multiple signal-plus-background fits are performed on a background-only template. These fits are repeated using different background models, such as exponential and power-law functions. In addition, different assumptions are made for the signal mass, with m_H varied between 123 and 127 GeV in steps of 0.5 GeV. The background-only template is constructed without accounting for misidentified photon backgrounds, as their contribution is found to have a negligible impact on the spurious signal estimate. For each of the background functions tested, the spurious signal is smaller than 20% of the statistical uncertainty in the expected fitted signal yield. The spurious signal value found in each category is taken as a systematic uncertainty in the signal yield.

The uncertainty in the full Run-2 integrated luminosity amounts to 0.83% [54]. The uncertainty in the Run-3 luminosity is estimated to be 4% and is uncorrelated with that of Run 2.

The uncertainty in the efficiency of the di-photon trigger in Run 2 and the 2022 dataset is estimated by using radiative Z boson decays and events from the pre-scaled lower threshold trigger [80], while for 2023 and 2024 the same trigger correction factors as in 2022 are employed, based on a study of the trigger efficiencies in data and simulation over the different years of the Run-3 data-taking. In Run 2, the photon identification and isolation uncertainties are determined using control samples of prompt photons from γ + jet production, radiative $Z \to \ell\ell\gamma$ decays, and electrons from $Z \to ee$ decays. In the latter case, electrons are used as a proxy for photons due to their similar calorimeter signatures [82]. The uncertainties in the photon energy scale and resolution in Run 2 are determined from control samples of electrons from Z boson decays and of photons from radiative Z boson decays [82]. The corresponding uncertainties for Run 3, in particular for the photon energy scale and resolution, are extrapolated from Run 2 [78].

The photon energy scale and resolution uncertainties affecting the peak and the width, respectively, of the signal and single Higgs boson background are estimated with both the SM ggF and VBF HH samples. The peak position has an uncertainty of less than 0.7% in all categories, while the uncertainty in the width is less than 21%. The photon energy scale and resolution effects on the yields are controlled by the same nuisance parameters as those on the $m_{\gamma\gamma}$ shape. The systematic uncertainties affecting the yields of processes with at least one Higgs boson are estimated separately for the ggF and VBF HH signals and the single Higgs boson production. For ggF and VBF HH production, experimental systematic uncertainties are estimated with the SM samples and applied to all HH configurations.

The uncertainties in the jet energy scale and resolution are estimated by using control samples in which jets recoil against well-calibrated reference objects, such as a photon or a Z boson, or other already calibrated jets [99]. An additional uncertainty is introduced in the simulation to account for variations in response among b-jets, light-quark jets, and gluon jets. The flavour tagging uncertainties include those arising from the efficiencies and misidentification rates. They are estimated in $t\bar{t}$ events for b- and c-jets, and in Z + jets events for light-quark and gluon jets [31,32,100].

For the ggF and VBF HH signal yield parameterisation, non-closure uncertainties are derived from the differences between the yields obtained from the parameterisation and simulated samples with different κ_λ, κ_{2V}, κ_V values. The maximal deviation over all samples is taken as the final uncertainty. In particular, the high-mass categories have a non-closure uncertainty of ∼10% that is comparable to Ref. [29]. The numbers in the low-mass regions are higher especially for the VBF HH sample, reaching up to ∼30%. However this does not noticeably affect the sensitivity, as VBF is subdominant to ggF in κ_λ measurements.

Theory uncertainties in the analysis impact both the acceptance and the cross sections. A key component of these is a 100% uncertainty applied to the yields of single Higgs boson production modes (ggF, VBF, and WH), motivated by studies of heavy-flavour production in association with top-quark pairs [101,102], W boson production in association with b-jets [103], and confirmed by measurements of single Higgs boson production in association with b-jets [104,105]. Other theory uncertainties originate from missing higher-order terms in perturbative QCD calculations and from the limited knowledge of PDFs and of the value of the strong coupling constant α_s. The uncertainty due to missing higher-order terms is evaluated by independently varying the renormalisation and factorisation scales. In the fit, all the theory uncertainties are correlated between Run 2 and Run 3, but uncorrelated between processes. These scale uncertainties are calculated separately for Run 2 and Run 3, in each category and for each process: for VBF production, they amount

Table 1
Impact of the various systematic uncertainties in the observed μ_{HH} measurement. For each uncertainty group, the error on μ_{HH} is obtained from a fit with only those corresponding nuisance parameters floating and all others fixed to their best-fit values. The impact is then calculated from the subtraction in quadrature of this error and the error when all nuisance parameters are fixed. The up (down) columns indicate the impact on the upper (lower) μ_{HH} error. When the up and down impacts are found to be compatible within 30%, the values are symmetrised in the table for better readability. Asymmetric impacts primarily result from the asymmetric QCD scale + m_{top} signal uncertainty, and the fact that the lower endpoint of the 68% CL error on the signal strength is close to 0. The heavy-flavour content uncertainty in the table refers to single Higgs boson production.

Source of systematic uncertainty	Relative impact (in %)	
	Up	Down
Experimental		
Photon energy scale	+22	−34
Photon energy resolution	+14	−7.5
Photon efficiency	+13	−2.5
Jet	+10	−6.9
Luminosity	+6.7	−1.2
Theory		
QCD scale + m_{top}, PDF + α_S	+35	−5.2
$\mathcal{B}(H \to \gamma\gamma, b\bar{b})$	+10	−2.1
Parton showering model	±15	
Heavy-flavour content	±30	
Background model		
Spurious signal	±7.2	

to 0.04%, while for ggF production, with the addition of the top-quark mass scheme uncertainty included according to Ref. [22], they amount to +6% and −23%.

The PDF and α_s uncertainties are estimated separately for Run 2 and Run 3 and separately for different processes (single Higgs boson, ggF HH and VBF HH events). The PDF + α_s uncertainties for the ggF (VBF) HH cross sections amount to 3.0% (2.1%). These uncertainties are evaluated for the SM case and their magnitude is parameterised in terms of κ_λ. The parton shower model uncertainty is estimated by using alternative simulation samples. In particular, for the HH and single Higgs boson processes the alternative samples use Herwig 7 [106,107] for parton showering.

In addition, branching ratio uncertainties are taken into account [108]. Specifically, for all HH and single Higgs boson processes, a 2.9% uncertainty is applied to the $H \to \gamma\gamma$ branching ratio. An additional 1.7% uncertainty from the $H \to b\bar{b}$ branching ratio is included for the HH signal.

The impact of the various systematic uncertainties on the observed μ_{HH} measurement is shown in Table 1. For each uncertainty group, the error on μ_{HH} is obtained from a fit with only those corresponding nuisance parameters floating and all others fixed to their best-fit values. The impact is then calculated from the subtraction in quadrature of this error and the error when all nuisance parameters are fixed. The up (down) columns indicate the impact of the upper (lower) μ_{HH} error. When the up and down variations are found to be compatible within 30%, the impacts are symmetrised in the table for better readability. Asymmetric impacts primarily result from the asymmetric QCD scale + m_{top} signal uncertainty, and the fact that the lower endpoint of the 68% CL error on the signal strength is close to 0. The heavy-flavour content uncertainty in the table refers to single Higgs boson production.

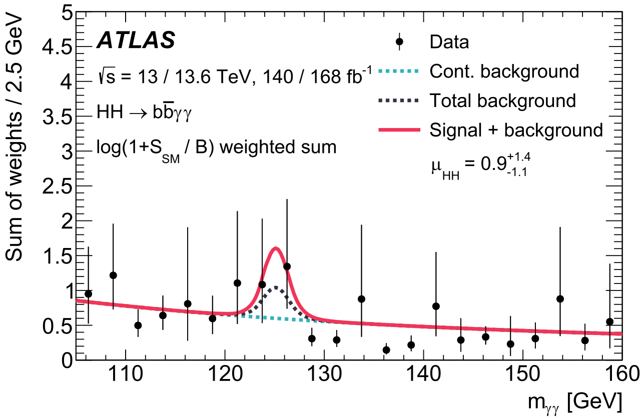

Fig. 5. Weighted di-photon invariant mass distribution summed over all categories and the two data-taking periods. The events in each category are weighted by $\log(1 + S_{\text{SM}}/B)$. S_{SM} is the expected signal yield assuming $\mu_{HH} = 1$, while B is the continuum background yield obtained from a fit to the sidebands plus the single Higgs boson background obtained from simulation, all in a ±5 GeV window around the Higgs boson mass. The lines show the fit results for the continuum background only (light dotted), adding single Higgs boson backgrounds (black dotted) and the full fit (solid).

7. Results

The search results are derived with a simultaneous profile-likelihood fit to the di-photon invariant mass distribution in all event categories, with a procedure similar to that described in Ref. [29]. The parameters of interest are fitted together with a set of nuisance parameters representing the systematic uncertainties, and the normalisation and shape of the continuum background. Uncertainties and confidence levels are derived using the asymptotic approximations [95], which agree within 10% with those from pseudo-experiments. Upper limits on the signal strength are derived using the CL_s approach [109]. It is always assumed that the Higgs boson satisfies exactly all SM predictions apart from the parameter under study.

Fig. 5 shows the di-photon invariant mass distribution summed over all categories and the two data-taking periods, where the events in each category are weighted by $\log(1 + S_{\text{SM}}/B)$, where S_{SM} is the expected signal yield assuming $\mu_{HH} = 1$, while B is the continuum background yield obtained from a fit to the sidebands plus the single Higgs boson background obtained from simulation, all in a 5 GeV window around the Higgs boson mass.

The best-fit value for the signal strength modifier is $\mu_{HH} = 0.9^{+1.4}_{-1.1} = 0.9^{+1.3}_{-1.0}\,(\text{stat.}) \pm 0.5\,(\text{syst.})$ for an expected value of $\mu_{HH} = 1^{+1.3}_{-1.0}$ in the SM. Fitting the data from Run 2 and Run 3 separately results in μ_{HH} values compatible with each other with a p-value of 0.40. The statistical significance for Higgs boson pair production is $0.78\,\sigma$, where $1.01\,\sigma$ is expected. The systematic uncertainty is dominated by the uncertainties in the heavy-flavour content in single Higgs boson production, the photon energy scale and resolution, and the calculation of the Higgs boson pair production cross section. An upper limit at 95% CL of $\mu_{HH} < 3.7$ is derived assuming SM HH kinematics. Assuming no HH production the expected limit is $\mu_{HH} < 2.6$, while assuming $\mu_{HH} = 1$, the expected limit becomes $\mu_{HH} < 3.7$. Fig. 6 compares the separate fit results for Run 2 and Run 3 as well as their combination in terms of the significance and the 95% CL upper limit. The same definition of the analysis categories is used for all fits. Compared to Ref. [29] the significance in μ_{HH} improved by approximately 20% due to the new b-tagging algorithm and an additional 5% comes from the kinematic fit. The improvement from the additional data is approximately 60%, with 50% attributed to increased statistics and 10% to the optimisation of the analysis categories, made possible by treating the background shapes in the two datasets as correlated.

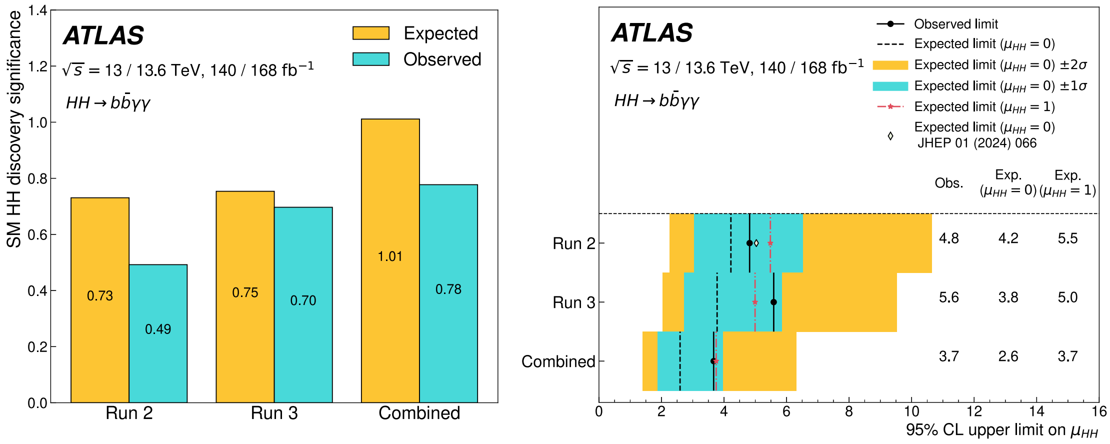

(a) (b)

Fig. 6. (a) Observed and expected statistical significance of the HH signal, and (b) the 95% CL upper limits on the signal strength, obtained with separate fits to Run-2 and Run-3 data as well as their combination. When computing the significance or upper limit for one data-taking period only, μ_{HH} of the other period is left free to vary. All other parameters of interest are fixed to their SM expectation. The expected limit assuming $\mu_{HH} = 0$ from Ref. [29] is also shown in (b).

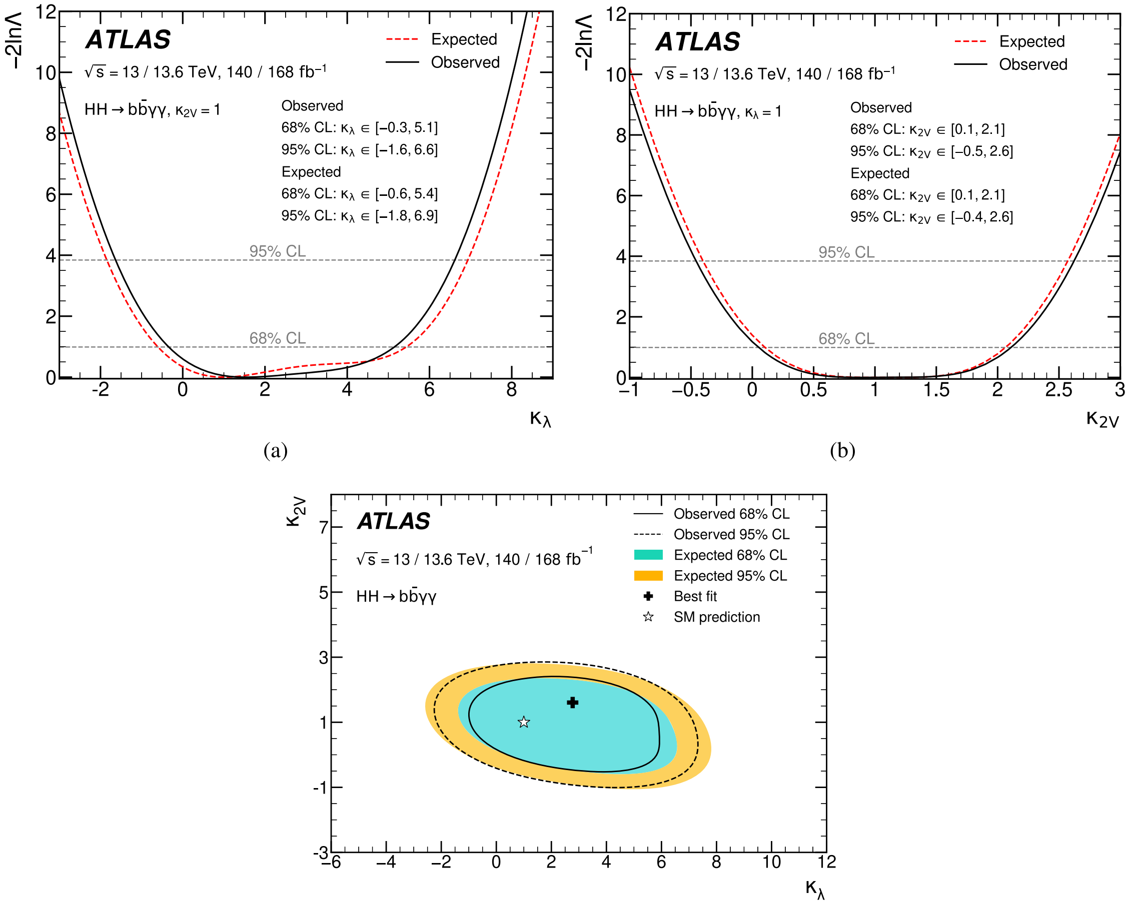

(c)

Fig. 7. Observed and expected profile likelihood scan of (a) κ_λ and (b) κ_{2V}. (c) Contours at 68% CL (solid line) and 95% CL (dashed line) in the $(\kappa_\lambda, \kappa_{2V})$ parameter space. The corresponding expected contours are shown by the inner and outer shaded regions. The SM prediction is indicated by the star, while the best-fit value is denoted by the cross. The scans are performed by varying only the coupling modifier of interest, while all other relevant coupling modifiers are fixed to unity. For the two-dimensional fit the individual results are $\kappa_\lambda = 2.8^{+2.2}_{-3.0}$ and $\kappa_{2V} = 1.6^{+0.6}_{-1.8}$, where the errors are one dimensional standard deviations.

Profile-likelihood fits are performed separately for the two coupling modifiers κ_λ and κ_{2V}, with all others fixed to their SM values. The likelihood scans are shown in Figs. 7(a) and 7(b). The best-fit values are $\kappa_\lambda = 1.4^{+3.7}_{-1.8}$ and $\kappa_{2V} = 0.9^{+1.2}_{-0.8}$, compatible with the expected values of $\kappa_\lambda = 1^{+4.4}_{-1.6}$ and $\kappa_{2V} = 1^{+1.1}_{-0.9}$. The observed (expected) 95% confidence intervals are $-1.6 < \kappa_\lambda < 6.6$ ($-1.8 < \kappa_\lambda < 6.9$) and $-0.5 < \kappa_{2V} < 2.6$ ($-0.4 < \kappa_{2V} < 2.6$). For these coupling modifiers, fits performed on the Run-2 and Run-3 data separately are compatible with p-values of 0.17 for κ_λ and 0.45 for κ_{2V}. Compared to Ref. [29], the expected width of the 95% confidence interval decreases by approximately 20% for κ_λ and 30% for κ_{2V}, respectively. The observed confidence intervals are similar to those in Ref. [29] due to differences in the observed best-fit values, which in Ref. [29] were driven by a small deficit of events in the signal region. A two-dimensional fit with κ_λ and κ_{2V} as free parameters yields observed and expected results of $\kappa_\lambda = 2.8^{+2.2}_{-3.0}$, $\kappa_{2V} = 1.6^{+0.6}_{-1.8}$, and $\kappa_\lambda = 1^{+4.7}_{-1.7}$, $\kappa_{2V} = 1^{+1.1}_{-1.3}$, respectively, where the other parameter is unconstrained when calculating the error. The central values and the 68% and 95% CL contours are shown in Fig. 7(c).

8. Conclusion

A search for Higgs boson pair production in the $b\bar{b}\gamma\gamma$ final state is performed. The proton–proton collision dataset used an integrated luminosity of 308 fb^{-1}, and consists of two samples, 140 fb^{-1} at a centre-of-mass energy of 13 TeV and 168 fb^{-1} at 13.6 TeV, recorded between 2015 and 2024 by the ATLAS detector at the CERN Large Hadron Collider. A simultaneous fit to all data in signal regions, categorised according to the $b\bar{b}\gamma\gamma$ invariant mass, signal purity, and data-taking period, results in a signal strength of $\mu_{HH} = 0.9^{+1.4}_{-1.1}$, compatible with the SM prediction of unity, and corresponding to an upper limit of $\mu_{HH} < 3.7$. Additional fits constrain the trilinear Higgs and $VVHH$ quartic couplings to $-1.6 < \kappa_\lambda < 6.6$ and $-0.5 < \kappa_{2V} < 2.6$, respectively, both at 95% confidence level. This new analysis improves the limit on the expected signal strength by almost a factor two assuming no HH production compared to the previous iteration based only on 13 TeV data [29].

Data availability

The data for this manuscript are not available. The values in the plots and tables associated to this article are stored in HEPDATA (http://hepdata.cedar.ac.uk)"

Acknowledgements

We thank CERN for the very successful operation of the LHC and its injectors, as well as the support staff at CERN and at our institutions worldwide without whom ATLAS could not be operated efficiently.

The crucial computing support from all WLCG partners is acknowledged gratefully, in particular from CERN, the ATLAS Tier-1 facilities at TRIUMF/SFU (Canada), NDGF (Denmark, Norway, Sweden), CC-IN2P3 (France), KIT/GridKA (Germany), INFN-CNAF (Italy), NL-T1 (Netherlands), PIC (Spain), RAL (UK) and BNL (USA), the Tier-2 facilities worldwide and large non-WLCG resource providers. Major contributors of computing resources are listed in Ref. [110].

We gratefully acknowledge the support of ANPCyT, Argentina; YerPhI, Armenia; ARC, Australia; BMWFW and FWF, Austria; ANAS, Azerbaijan; CNPq and FAPESP, Brazil; NSERC, NRC and CFI, Canada; CERN; ANID, Chile; CAS, MOST and NSFC, China; Minciencias, Colombia; MEYS CR, Czech Republic; DNRF and DNSRC, Denmark; IN2P3-CNRS and CEA-DRF/IRFU, France; SRNSFG, Georgia; BMFTR, HGF and MPG, Germany; GSRI, Greece; RGC and Hong Kong SAR, China; ICHEP and Academy of Sciences and Humanities, Israel; INFN, Italy; MEXT and JSPS, Japan; CNRST, Morocco; NWO, Netherlands; RCN, Norway; MNiSW, Poland; FCT, Portugal; MNE/IFA, Romania; MSTDI, Serbia; MSSR, Slovakia; ARIS and MVZI, Slovenia; DSI/NRF, South Africa; MICIU/AEI, Spain; SRC and Wallenberg Foundation, Sweden; SERI, SNSF and Cantons of Bern and Geneva, Switzerland; NSTC, Taipei; TENMAK, Türkiye; STFC/UKRI, United Kingdom; DOE and NSF, United States of America.

Individual groups and members have received support from BCKDF, CANARIE, CRC and DRAC, Canada; CERN-CZ, FORTE and PRIMUS, Czech Republic; COST, ERC, ERDF, Horizon 2020, ICSC-NextGenerationEU and Marie Skłodowska-Curie Actions, European Union; Investissements d'Avenir Labex, Investissements d'Avenir Idex and ANR, France; DFG and AvH Foundation, Germany; Herakleitos, Thales and Aristeia programmes co-financed by EU-ESF and the Greek NSRF, Greece; BSF-NSF and MINERVA, Israel; NCN and NAWA, Poland; La Caixa Banking Foundation, CERCA Programme Generalitat de Catalunya and PROMETEO and GenT Programmes Generalitat Valenciana, Spain; Göran Gustafssons Stiftelse, Sweden; The Royal Society and Leverhulme Trust, United Kingdom; United States of America.

In addition, individual members wish to acknowledge support from CERN: European Organization for Nuclear Research (CERN DOCT); Chile: Agencia Nacional de Investigación y Desarrollo (ANID FONDECYT reg. 1230987, FONDECYT 1230812, FONDECYT 1240864, Fondecyt 3240661, Fondecyt Regular 1240721); China: Chinese Ministry of Science and Technology (MOST-2023YFA1605700, MOST-2023YFA1609300), National Natural Science Foundation of China (NSFC - 12175119, NSFC 12275265); Czech Republic: Czech Science Foundation (GACR - 24-11373S), Ministry of Education Youth and Sports (ERC-CZ-LL2327, FORTE CZ.02.01.01/00/22_008/0004632), PRIMUS Research Programme (PRIMUS/21/SCI/017); EU: H2020 European Research Council (ERC - 101002463); European Union: European Research Council (BARD No. 101116429, ERC - 948254, ERC 101089007), European Regional Development Fund (HE COFUND GA No. 101081355, ERDF), Horizon 2020 Framework Programme (MUCCA - CHIST-ERA-19-XAI-00), European Union, Future Artificial Intelligence Research (FAIR-NextGenerationEU PE00000013), Italian Center for High Performance Computing, Big Data and Quantum Computing (ICSC, NextGenerationEU); France: Agence Nationale de la Recherche (ANR-21-CE31-0013, ANR-21-CE31-0022, ANR-22-EDIR-0002, ANR-24-CE31-0504-01); Germany: Baden-Württemberg Stiftung (BW Stiftung-Postdoc Eliteprogramme), Deutsche Forschungsgemeinschaft (DFG - 469666862, DFG - CR 312/5-2); China: Research Grants Council (GRF); Italy: Istituto Nazionale di Fisica Nucleare (ICSC, NextGenerationEU), Ministero dell'Università e della Ricerca (NextGenEU 153D23001490006 M4C2.1.1, NextGenEU I53D23000820006 M4C2.1.1, NextGenEU I53D23001490006 M4C2.1.1, SOE2024_0000023); Japan: Japan Society for the Promotion of Science (JSPS KAKENHI JP22H01227, JSPS KAKENHI JP22H04944, JSPS KAKENHI JP22KK0227, JSPS KAKENHI JP24K23939, JSPS KAKENHI JP24KK0251, JSPS KAKENHI JP25H00650, JSPS KAKENHI JP25H01291, JSPS KAKENHI JP25K01023); Norway: Research Council of Norway (RCN-314472); Poland: Ministry of Science and Higher Education (IDUB AGH, POB8, D4 no 9722), Polish National Science Centre (NCN 2021/42/E/ST2/00350, NCN OPUS 2023/51/B/ST2/02507, NCN OPUS nr 2022/47/B/ST2/03059, NCN UMO-2019/34/E/ST2/00393, UMO-2022/47/O/ST2/00148, UMO-2023/49/B/ST2/04085, UMO-2023/51/B/ST2/00920, UMO-2024/53/N/ST2/00869); Portugal: Foundation for Science and Technology (FCT); Spain: Agencia de Gestión de Ayudas Universitarias y de Investigación (AGAUR - 2023 BP 00141), Generalitat Valenciana (ASFAE/2022/008), Ministry of Science and Innovation (MCIN & NextGenEU PCI2022-135018-2, MICIN & FEDER PID2021-125273NB, RYC2019-028510-I, RYC2020-030254-I, RYC2021-031273-I, RYC2022-038164-I), Ministerio de Ciencia, Innovación y Universidades/Agencia Estatal de Investigación (PID2022-142604OB-C22); Sweden: Carl Trygger Foundation (Carl Trygger Foundation CTS 22:2312), Swedish Research Council (Swedish Research Council 2023-04654, VR

2021-03651, VR 2022-03845, VR 2022-04683, VR 2023-03403, VR 2024-05451), Knut and Alice Wallenberg Foundation (KAW 2018.0458, KAW 2022.0358, KAW 2023.0366); Switzerland: Swiss National Science Foundation (SNSF - PCEFP2_194658); United Kingdom: Royal Society (NIF-R1-231091); United States of America: U.S. Department of Energy (ECA DE-AC02-76SF00515), Neubauer Family Foundation.

Declaration of competing interest

The authors declare that they have no known competing financial interests or personal relationships that could have appeared to influence the work reported in this paper.

Appendix

The ATLAS Collaboration

G. Aad[152], E. Aakvaag[18], B. Abbott[174], S. Abdelhameed[169], K. Abeling[82], N.J. Abicht[76], S.H. Abidi[43], M. Aboelela[71], A. Aboulhorma[60], H. Abramowicz[224], Y. Abulaiti[171], B.S. Acharya[XIV,100,101], A. Ackermann[91], C. Adam Bourdarios[5], L. Adamczyk[134], S.V. Addepalli[214], M.J. Addison[151], J. Adelman[168], A. Adiguzel[26], T. Adye[194], A.A. Affolder[196], Y. Afik[65], M.N. Agaras[14], A. Aggarwal[150], C. Agheorghiesei[36], F. Ahmadov[XXXI,64], S. Ahuja[145], X. Ai[207], G. Aielli[115,116], A. Aikot[237], M. Ait Tamlihat[60], B. Aitbenchikh[56], M. Akbiyik[150], T.P.A. Åkesson[148], A.V. Akimov[216], D. Akiyama[242], N.N. Akolkar[31], S. Aktas[240], G.L. Alberghi[30], J. Albert[239], U. Alberti[22], P. Albicocco[80], G.L. Albouy[88], S. Alderweireldt[79], Z.L. Alegria[175], M. Aleksa[62], I.N. Aleksandrov[64], C. Alexa[35], T. Alexopoulos[11], F. Alfonsi[30], M. Algren[83], M. Alhroob[241], B. Ali[192], H.M.J. Ali[XXIV,141], S. Ali[45], S.W. Alibocus[142], M. Aliev[49], G. Alimonti[105], W. Alkakhi[82], C. Allaire[97], B.M.M. Allbrooke[217], J.S. Allen[151], J.F. Allen[79], P.P. Allport[23], A. Aloisio[107,108], F. Alonso[140], C. Alpigiani[205], Z.M.K. Alsolami[141], A. Alvarez Fernandez[150], M. Alves Cardoso[83], M.G. Alviggi[107,108], M. Aly[151], Y. Amaral Coutinho[126], A. Ambler[154], C. Amelung[62], M. Amerl[151], C.G. Ames[159], T. Amezza[181], D. Amidei[156], B. Amini[81], K. Amirie[228], A. Amirkhanov[64], S.P. Amor Dos Santos[184], K.R. Amos[237], D. Amperiadou[225], S. An[130], C. Anastopoulos[210], T. Andeen[12], J.K. Anders[142], A.C. Anderson[87], A. Andreazza[105,106], S. Angelidakis[10], A. Angerami[67], A.V. Anisenkov[64], A. Annovi[111], C. Antel[62], E. Antipov[216], M. Antonelli[80], F. Anulli[113], M. Aoki[130], T. Aoki[226], M.A. Aparo[217], L. Aperio Bella[75], M. Apicella[44], C. Appelt[224], A. Apyan[33], M. Arampatzi[11], S.J. Arbiol Val[136], C. Arcangeletti[80], A.T.H. Arce[78], J-F. Arguin[158], S. Argyropoulos[225], J.-H. Arling[75], O. Arnaez[5], H. Arnold[216], G. Artoni[113,114], H. Asada[161], K. Asai[172], S. Asatryan[247], N.A. Asbah[62], R.A. Ashby Pickering[241], A.M. Aslam[145], K. Assamagan[43], R. Astalos[41], K.S.V. Astrand[148], S. Atashi[233], R.J. Atkin[47], H. Atmani[61], P.A. Atmasiddha[182], K. Augsten[192], A.D. Auriol[66], V.A. Austrup[151], A.S. Avad[144], G. Avolio[62], K. Axiotis[83], A. Azzam[14], D. Babal[42], H. Bachacou[195], K. Bachas[XVIII,225], A. Bachiu[55], E. Bachmann[77], M.J. Backes[91], A. Badea[65], T.M. Baer[156], P. Bagnaia[113,114], M. Bahmani[21], D. Bahner[81], K. Bai[177], J.T. Baines[194], L. Baines[144], O.K. Baker[246], E. Bakos[17], D. Bakshi Gupta[9], L.E. Balabram Filho[126], V. Balakrishnan[174], R. Balasubramanian[5], E.M. Baldin[63], P. Balek[134], E. Ballabene[30,29], F. Balli[195], L.M. Baltes[91], W.K. Balunas[46], J. Balz[150], I. Bamwidhi[170], E. Banas[136], M. Bandieramonte[183], A. Bandyopadhyay[31], S. Bansal[31], L. Barak[224], M. Barakat[75], E.L. Barberio[155], D. Barberis[20], M. Barbero[152], M.Z. Barel[167], T. Barillari[160], M-S. Barisits[62], T. Barklow[214], P. Baron[193], D.A. Baron Moreno[151], A. Baroncelli[90], A.J. Barr[180], J.D. Barr[146], F. Barreiro[149], J. Barreiro Guimarães da Costa[15], M.G. Barros Teixeira[184], S. Barsov[63], F. Bartels[91], R. Bartoldus[214], A.E. Barton[141], P. Bartos[41], M. Baselga[76], S. Bashiri[136], A. Bassalat[III,97], M.J. Basso[229], S. Bataju[71], R. Bate[238], R.L. Bates[87], S. Batlamous[149], M. Battaglia[196], D. Battulga[21], M. Bauce[113,114], M. Bauer[121], P. Bauer[31], L.T. Bayer[75], L.T. Bazzano Hurrell[44], J.B. Beacham[160], T. Beau[181], J.Y. Beaucamp[140], P.H. Beauchemin[232], P. Bechtle[31], H.P. Beck[XVII,22], K. Becker[241], A.J. Beddall[124], V.A. Bednyakov[64], C.P. Bee[216], L.J. Beemster[17], M. Begalli[128], M. Begel[43], J.K. Behr[75], J.F. Beirer[62], F. Beisiegel[31], M. Belfkir[170], G. Bella[224], L. Bellagamba[30], A. Bellerive[55], C.D. Bellgraph[99], P. Bellos[23], K. Beloborodov[63], I. Benaoumeur[23], D. Benchekroun[56], F. Bendebba[56], Y. Benhammou[224], K.C. Benkendorfer[89], L. Beresford[75], M. Beretta[80], E. Bergeaas Kuutmann[235], N. Berger[5], B. Bergmann[192], J. Beringer[19], G. Bernardi[6], C. Bernius[214], F.U. Bernlochner[31], A. Berrocal Guardia[14], T. Berry[145], P. Berta[193], A. Berthold[77], A. Berti[184], R. Bertrand[152], S. Bethke[160], A. Betti[113,114], A.J. Bevan[144], L. Bezio[83], N.K. Bhalla[81], S. Bharthuar[160], S. Bhatta[216], P. Bhattarai[214], Z.M. Bhatti[171], K.D. Bhide[81], V.S. Bhopatkar[175], R.M. Bianchi[183], G. Bianco[30,29], O. Biebel[159], M. Biglietti[117], C.S. Billingsley[71], Y. Bimgdi[61], M. Bindi[82], A. Bingham[245], A. Bingul[25], C. Bini[113,114], G.A. Bird[46], M. Birman[243], M. Biros[193], S. Biryukov[217], T. Bisanz[76], E. Bisceglie[30,29], J.P. Biswal[194], D. Biswas[212], I. Bloch[75], A. Blue[87], U. Blumenschein[144], V.S. Bobrovnikov[64], L. Boccardo[85,84], M. Boehler[81], B. Boehm[240], D. Bogavac[14], A.G. Bogdanchikov[63], L.S. Boggia[181], V. Boisvert[145], P. Bokan[62], T. Bold[134], M. Bomben[6], M. Bona[144], M. Boonekamp[195], A.G. Borbély[87], I.S. Bordulev[63], G. Borissov[141], D. Bortoletto[180], D. Boscherini[30], M. Bosman[14], K. Bouaouda[56], N. Bouchhar[237], L. Boudet[5], J. Boudreau[183], E.V. Bouhova-Thacker[141], D. Boumediene[66], R. Bouquet[85,84], A. Boveia[173], J. Boyd[62], D. Boye[43], I.R. Boyko[64], L. Bozianu[83], J. Bracinik[23], N. Brahimi[5], G. Brandt[245], O. Brandt[46], B. Brau[153], J.E. Brau[177], R. Brener[243], L. Brenner[167], R. Brenner[235], S. Bressler[243], G. Brianti[119,120], D. Britton[87], D. Britzger[160], I. Brock[31], R. Brock[157], G. Brooijmans[67], A.J. Brooks[99], E.M. Brooks[230], E. Brost[43], L.M. Brown[239,229], L.E. Bruce[89], T.L. Bruckler[180], P.A. Bruckman de Renstrom[136], B. Brüers[75], A. Bruni[30], G. Bruni[30], D. Brunner[73,74], M. Bruschi[30], N. Bruscino[113,114], T. Buanes[18], Q. Buat[205], D. Buchin[160], A.G. Buckley[87], O. Bulekov[124], B.A. Bullard[214], S. Burdin[142], C.D. Burgard[76], A.M. Burger[139], B. Burghgrave[9], O. Burlayenko[81], J. Burleson[236], J.C. Burzynski[213], E.L. Busch[67], V. Büscher[150], P.J. Bussey[87], J.M. Butler[32], C.M. Buttar[87], J.M. Butterworth[146], W. Buttinger[194], C.J. Buxo Vazquez[157], A.R. Buzykaev[64], S. Cabrera Urbán[237], L. Cadamuro[97], H. Cai[62], Y. Cai[30,164,29], Y. Cai[162], V.M.M. Cairo[62], O. Cakir[3], N. Calace[62], P. Calafiura[19], G. Calderini[181], P. Calfayan[55], L. Calic[148], G. Callea[87], L.P. Caloba[126], D. Calvet[66], S. Calvet[66], R. Camacho Toro[181], S. Camarda[62], D. Camarero Munoz[33], P. Camarri[115,116], C. Camincher[239], M. Campanelli[146], A. Camplani[68], V. Canale[107,108], A.C. Canbay[3], E. Canonero[145], J. Cantero[237], Y. Cao[236], F. Capocasa[33], M. Capua[70,69], A. Carbone[105,106], R. Cardarelli[115], J.C.J. Cardenas[9], M.P. Cardiff[33], G. Carducci[70,69], T. Carli[62], G. Carlino[107], J.I. Carlotto[14], B.T. Carlson[XIX,183], E.M. Carlson[239], J. Carmignani[142], L. Carminati[105,106], A. Carnelli[5], M. Carnesale[62], S. Caron[166], E. Carquin[203], I.B. Carr[155], S. Carrá[109,110], G. Carratta[30,29], C. Carrion Martinez[237], A.M. Carroll[177], M.P. Casado[IX,14], P. Casolaro[107,108], M. Caspar[75], W.R. Castiglioni[65], F.L. Castillo[5], L. Castillo Garcia[14], V. Castillo Gimenez[237], N.F. Castro[184,188], A. Catinaccio[62], J.R. Catmore[179], T. Cavaliere[5], V. Cavaliere[43], L.J. Caviedes Betancourt[28], E. Celebi[124], S. Cella[62], V. Cepaitis[83], K. Cerny[176], A.S. Cerqueira[125], A. Cerri[XL,111], L. Cerrito[115,116], F. Cerutti[19], B. Cervato[105,106], A. Cervelli[30], G. Cesarini[80], S.A. Cetin[124], P.M. Chabrillat[181], R. Chakkappai[97], S. Chakraborty[241], A. Chambers[89], J. Chan[19], W.Y. Chan[226], J.D. Chapman[46], E. Chapon[195], B. Chargeishvili[221], D.G. Charlton[23], C. Chauhan[193], Y. Che[162], S. Chekanov[7], S.V. Chekulaev[229], G.A. Chelkov[II,64],

B. Chen[224], B. Chen[239], H. Chen[162], H. Chen[43], J. Chen[208], J. Chen[213], M. Chen[180], S. Chen[137], S.J. Chen[162], X. Chen[208], X. Chen[XXXV,16], Z. Chen[90], C.L. Cheng[244], H.C. Cheng[93], S. Cheong[214], A. Cheplakov[64], E. Cherepanova[167], R. Cherkaoui El Moursli[60], E. Cheu[8], K. Cheung[96], L. Chevalier[195], V. Chiarella[80], G. Chiarelli[111], G. Chiodini[103], A.S. Chisholm[23], A. Chitan[35], M. Chitishvili[237], M.V. Chizhov[XX,64], K. Choi[12], Y. Chou[205], E.Y.S. Chow[166], K.L. Chu[243], M.C. Chu[93], X. Chu[15,164], Z. Chubinidze[80], J. Chudoba[191], J.J. Chwastowski[136], D. Cieri[160], K.M. Ciesla[134], V. Cindro[143], A. Ciocio[19], F. Cirotto[107,108], Z.H. Citron[243], M. Citterio[105], D.A. Ciubotaru[35], A. Clark[83], P.J. Clark[79], N. Clarke Hall[146], C. Clarry[228], S.E. Clawson[75], C. Clement[73,74], Y. Coadou[152], M. Cobal[100,102], A. Coccaro[85], R.F. Coelho Barrue[184], R. Coelho Lopes De Sa[153], S. Coelli[105], L.S. Colangeli[228], B. Cole[67], P. Collado Soto[149], J. Collot[88], M.R. Coluccia[103], P. Conde Muiño[184,190], M.P. Connell[49], S.H. Connell[49], E.I. Conroy[180], M. Contreras Cossio[12], F. Conventi[XXXVII,107], A.M. Cooper-Sarkar[180], L. Corazzina[113,114], F.A. Corchia[30,29], A. Cordeiro Oudot Choi[205], L.D. Corpe[66], M. Corradi[113,114], F. Corriveau[XXIX,154], A. Cortes-Gonzalez[226], M.J. Costa[237], F. Costanza[5], D. Costanzo[210], J. Couthures[5], G. Cowan[145], T. Cozzi[106], K. Cranmer[244], L. Cremer[76], D. Cremonini[30,29], S. Crépé-Renaudin[88], F. Crescioli[181], T. Cresta[109,110], M. Cristinziani[212], M. Cristoforetti[119,120], V. Croft[167], G. Crosetti[70,69], A. Cueto[149], H. Cui[146], Z. Cui[8], B.M. Cunnett[217], W.R. Cunningham[87], F. Curcio[237], J.R. Curran[79], M.J. Da Cunha Sargedas De Sousa[85,84], J.V. Da Fonseca Pinto[126], C. Da Via[151], W. Dabrowski[134], T. Dado[62], S. Dahbi[219], T. Dai[156], D. Dal Santo[22], C. Dallapiccola[153], M. Dam[68], G. D'amen[43], V. D'Amico[159], J. Damp[150], J.R. Dandoy[55], M. D'Andrea[85,84], D. Dannheim[62], G. D'anniballe[111,112], M. Danninger[213], V. Dao[216], G. Darbo[85], S.J. Das[43], F. Dattola[75], S. D'Auria[105,106], A. D'Avanzo[107,108], T. Davidek[193], J. Davidson[241], I. Dawson[144], K. De[9], C. De Almeida Rossi[228], R. De Asmundis[107], N. De Biase[75], S. De Castro[30,29], N. De Groot[166], P. de Jong[167], H. De la Torre[168], A. De Maria[162], A. De Salvo[113], U. De Sanctis[115,116], F. De Santis[103,104], A. De Santo[217], J.B. De Vivie De Regie[88], J. Debevc[143], D.V. Dedovich[64], J. Degens[142], A.M. Deiana[71], J. Del Peso[149], L. Delagrange[181], F. Deliot[195], C.M. Delitzsch[76], M. Della Pietra[107,108], D. Della Volpe[83], A. Dell'Acqua[62], L. Dell'Asta[105,106], M. Delmastro[5], C.C. Delogu[150], P.A. Delsart[88], S. Demers[246], M. Demichev[64], S.P. Denisov[63], H. Denizli[XIII,24], L. D'Eramo[66], D. Derendarz[136], F. Derue[181], P. Dervan[I,142], A.M. Desai[1], K. Desch[31], F.A. Di Bello[85,84], A. Di Ciaccio[115,116], L. Di Ciaccio[5], A. Di Domenico[113,114], C. Di Donato[107,108], A. Di Girolamo[62], G. Di Gregorio[62], A. Di Luca[119,120], B. Di Micco[117,118], R. Di Nardo[117,118], K.F. Di Petrillo[65], M. Diamantopoulou[55], F.A. Dias[167], M.A. Diaz[197,198], A.R. Didenko[64], M. Didenko[237], S.D. Diefenbacher[19], E.B. Diehl[156], S. Díez Cornell[75], C. Diez Pardos[212], C. Dimitriadi[215], A. Dimitrievska[23], A. Dimri[216], Y. Ding[90], J. Dingfelder[31], T. Dingley[180], I-M. Dinu[35], S.J. Dittmeier[92], F. Dittus[62], M. Divisek[193], B. Dixit[142], F. Djama[152], T. Djobava[221], C. Doglioni[151,148], A. Dohnalova[41], Z. Dolezal[193], K. Domijan[134], K.M. Dona[65], M. Donadelli[128], B. Dong[157], J. Donini[66], A. D'Onofrio[107,108], M. D'Onofrio[142], J. Dopke[194], A. Doria[107], N. Dos Santos Fernandes[184], I.A. Dos Santos Luz[129], P. Dougan[151], M.T. Dova[140], A.T. Doyle[87], M.P. Drescher[82], E. Dreyer[243], I. Drivas-koulouris[11], M. Drnevich[171], D. Du[90], T.A. du Pree[167], Z. Duan[162], M. Dubau[5], F. Dubinin[64], M. Dubovsky[41], E. Duchovni[243], G. Duckeck[159], P.K. Duckett[146], O.A. Ducu[35], D. Duda[79], A. Dudarev[62], M.M. Dudek[136], E.R. Duden[33], M. D'uffizi[151], L. Duflot[97], M. Dührssen[62], I. Duminica[40], A.E. Dumitriu[35], M. Dunford[91], K. Dunne[73,74], A. Duperrin[152], H. Duran Yildiz[3], A. Durglishvili[221], G.I. Dyckes[19], M. Dyndal[134], B.S. Dziedzic[62], Z.O. Earnshaw[217], G.H. Eberwein[180], B. Eckerova[41], S. Eggebrecht[82], E. Egidio Purcino De Souza[129], G. Eigen[18], K. Einsweiler[19], T. Ekelof[235], P.A. Ekman[148], S. El Farkh[57], Y. El Ghazali[90], H. El Jarrari[62], A. El Moussaouy[56], D. Elitez[62], M. Ellert[235], F. Ellinghaus[245], T.A. Elliot[145], N. Ellis[62], J. Elmsheuser[43], M. Elsawy[169], M. Elsing[62], D. Emeliyanov[194], Y. Enari[130], S. Epari[158], D. Ernani Martins Neto[136], F. Ernst[62], M. Errenst[245], M. Escalier[97], C. Escobar[237], E. Etzion[224], G. Evans[184,185], H. Evans[99], L.S. Evans[75], A. Ezhilov[63], S. Ezzarqtouni[56], F. Fabbri[30,29], L. Fabbri[30,29], G. Facini[146], V. Fadeyev[196], R.M. Fakhrutdinov[63], D. Fakoudis[150], S. Falciano[113], L.F. Falda Ulhoa Coelho[184], F. Fallavollita[160], G. Falsetti[70,69], J. Faltova[193], C. Fan[236], K.Y. Fan[94], Y. Fan[15], Y. Fang[15,164], M. Fanti[105,106], M. Faraj[100,101], Z. Farazpay[147], A. Farbin[9], A. Farilla[117], K. Farman[219], T. Farooque[157], J.N. Farr[246], S.M. Farrington[194,79], F. Fassi[60], D. Fassouliotis[10], L. Fayard[97], P. Federic[193], P. Federicova[191], O.L. Fedin[II,63], M. Feickert[244], L. Feligioni[152], D.E. Fellers[19], C. Feng[206], Y. Feng[15], Z. Feng[167], M.J. Fenton[233], L. Ferencz[75], B. Fernandez Barbadillo[141], P. Fernandez Martinez[98], M.J.V. Fernoux[152], J. Ferrando[141], A. Ferrari[235], P. Ferrari[167,166], R. Ferrari[109], D. Ferrere[83], C. Ferretti[156], M.P. Fewell[1], D. Fiacco[113,114], F. Fiedler[150], P. Fiedler[192], S. Filimonov[64], M.S. Filip[XXI,35], A. Filipčič[143], E.K. Filmer[229], F. Filthaut[166], M.C.N. Fiolhais[IV,184,186], L. Fiorini[237], W.C. Fisher[157], T. Fitschen[151], P.M. Fitzhugh[195], I. Fleck[212], P. Fleischmann[156], T. Flick[245], M. Flores[XXXIV,50], L.R. Flores Castillo[93], L. Flores Sanz De Acedo[62], F.M. Follega[119,120], N. Fomin[46], J.H. Foo[228], A. Formica[195], A.C. Forti[151], E. Fortin[62], A.W. Fortman[19], L. Foster[19], L. Fountas[X,10], D. Fournier[97], H. Fox[141], P. Francavilla[111,112], S. Francescato[89], S. Franchellucci[83], M. Franchini[30,29], S. Franchino[91], D. Francis[62], L. Franco[166], L. Franconi[75], M. Franklin[89], G. Frattari[33], Y.Y. Frid[224], J. Friend[87], N. Fritzsche[62], A. Froch[83], D. Froidevaux[62], J.A. Frost[180], Y. Fu[157], S. Fuenzalida Garrido[203], M. Fujimoto[216], K.Y. Fung[93], E. Furtado De Simas Filho[129], M. Furukawa[226], J. Fuster[237], A. Gaa[82], A. Gabrielli[30,29], A. Gabrielli[228], P. Gadow[62], G. Gagliardi[85,84], L.G. Gagnon[19], S. Gaid[132], S. Galantzan[224], J. Gallagher[1], E.J. Gallas[180], A.L. Gallen[235], B.J. Gallop[194], K.K. Gan[173], S. Ganguly[226], Y. Gao[79], A. Garabaglu[205], F.M. Garay Walls[197,198], C. García[237], A. Garcia Alonso[167], A.G. Garcia Caffaro[246], J.E. García Navarro[237], M.A. Garcia Ruiz[28], M. Garcia-Sciveres[19], G.L. Gardner[182], R.W. Gardner[65], N. Garelli[232], R.B. Garg[214], J.M. Gargan[46], C.A. Garner[228], C.M. Garvey[47], V.K. Gassmann[232], G. Gaudio[109], V. Gautam[14], P. Gauzzi[113,114], J. Gavranovic[143], I.L. Gavrilenko[184], A. Gavrilyuk[63], C. Gay[238], G. Gaycken[177], E.N. Gazis[11], A. Gekow[173], C. Gemme[85], M.H. Genest[88], A.D. Gentry[165], S. George[145], T. Geralis[72], A.A. Gerwin[174], P. Gessinger-Befurt[62], M.E. Geyik[245], M. Ghani[241], K. Ghorbanian[144], A. Ghosal[212], A. Ghosh[233], A. Ghosh[8], B. Giacobbe[30], S. Giagu[113,114], T. Giani[167], A. Giannini[90], S.M. Gibson[145], M. Gignac[196], D.T. Gil[135], A.K. Gilbert[134], B.J. Gilbert[67], D. Gillberg[55], G. Gilles[167], D.M. Gingrich[XXXVI,2], M.P. Giordani[100,102], P.F. Giraud[195], G. Giugliarelli[100,102], D. Giugni[105], F. Giuli[115,116], I. Gkialas[X,10], L.K. Gladilin[63], C. Glasman[149], M. Glazewska[22], R.M. Gleason[233], G. Glemža[75], M. Glisic[177], I. Gnesi[70], Y. Go[43], M. Goblirsch-Kolb[62], B. Gocke[76], D. Godin[158], B. Gokturk[24], S. Goldfarb[155], T. Golling[83], M.G.D. Gololo[49], D. Golubkov[63], J.P. Gombas[157], A. Gomes[184,185], G. Gomes Da Silva[212], A.J. Gomez Delegido[62], R. Gonçalo[184], L. Gonella[23], A. Gongadze[222], F. Gonnella[23], J.L. Gonski[214], R.Y. González Andana[79], S. González de la Hoz[237], M.V. Gonzalez Rodrigues[75], R. Gonzalez Suarez[235], S. Gonzalez-Sevilla[83], L. Goossens[62], B. Gorini[62], E. Gorini[103,104], A. Gorišek[143], T.C. Gosart[182], A.T. Goshaw[78], M.I. Gostkin[64], S. Goswami[175], C.A. Gottardo[62], S.A. Gotz[159], M. Gouighri[57], A.G. Goussiou[205], N. Govender[49], R.P. Grabarczyk[180], I. Grabowska-Bold[134], K. Graham[55], E. Gramstad[179], S. Grancagnolo[103,104], C.M. Grant[1], P.M. Gravila[39], F.G. Gravili[103,104], H.M. Gray[19], M. Greco[160], M.J. Green[1], C. Grefe[31], A.S. Grefsrud[18], I.M. Gregor[75], K.T. Greif[233], P. Grenier[214], S.G. Grewe[160], A.A. Grillo[196], K. Grimm[45], S. Grinstein[XXV,14], J.-F. Grivaz[97], E. Gross[243], J. Grosse-Knetter[82], L. Guan[156], G. Guerrieri[62], R. Guevara[179], R. Gugel[150], J.A.M. Guhit[156], A. Guida[21], E. Guilloton[241], S. Guindon[62], F. Guo[15,164], J. Guo[208], L. Guo[75], L. Guo[XXIII,163], Y. Guo[156], Y. Guo[67], A. Gupta[76], R. Gupta[183], S. Gupta[33], S. Gurbuz[31], S.S. Gurdasani[75], G. Gustavino[113,114], P. Gutierrez[174], L.F. Gutierrez Zagazeta[182], M. Gutsche[77], C. Gutschow[146], C. Gwenlan[180], C.B. Gwilliam[142], E.S. Haaland[179], A. Haas[171], M. Habedank[87], C. Haber[19], H.K. Hadavand[9], A. Haddad[66], A. Hadef[77], A.I. Hagan[141], J.J. Hahn[212], E.H. Haines[146], M. Haleem[240], J. Haley[175], G.D. Hallewell[152], K. Hamano[239], H. Hamdaoui[235], M. Hamer[31], S.E.D. Hammoud[97], E.J. Hampshire[145], J. Han[206], L. Han[162], L. Han[90], S. Han[15], K. Hanagaki[130], M. Hance[196], D.A. Hangal[67], H. Hanif[213], M.D. Hank[182], J.B. Hansen[68], P.H. Hansen[68], D. Harada[83], T. Harenberg[245], S. Harkusha[247], M.L. Harris[153], Y.T. Harris[31], J. Harrison[14], N.M. Harrison[173], P.F. Harrison[241], M.L.E. Hart[146], N.M. Hartman[160], N.M. Hartmann[159], R.Z. Hasan[145,194], Y. Hasegawa[211], F. Haslbeck[180], S. Hassan[18], R. Hauser[157], M. Haviernik[193], C.M. Hawkes[23], R.J. Hawkings[62], Y. Hayashi[226], D. Hayden[157], C. Hayes[156], R.L. Hayes[167], C.P. Hays[180], J.M. Hays[144], H.S. Hayward[142], M. He[15,164], Y. He[75], Y. He[146], N.B. Heatley[144], V. Hedberg[148], C. Heidegger[81], K.K. Heidegger[81], J. Heilman[55], S. Heim[75], T. Heim[19], J.J. Heinrich[177], L. Heinrich[160], J. Hejbal[191], M. Helbig[77], A. Held[244], S. Hellesund[18], C.M. Helling[238], S. Hellman[73,74], A.M. Henriques Correia[62], H. Herde[148], Y. Hernández Jiménez[216], L.M. Herrmann[31], T. Herrmann[77], G. Herten[81], R. Hertenberger[159], L. Hervas[62], M.E. Hesping[150], N.P. Hessey[229], J. Hessler[160], M. Hidaoui[57], N. Hidic[193], E. Hill[228], T.S. Hillersoy[18], S.J. Hillier[23], J.R. Hinds[157], F. Hinterkeuser[31], M. Hirose[178], S. Hirose[231], D. Hirschbuehl[245], T.G. Hitchings[151], B. Hiti[143], J. Hobbs[216], R. Hobincu[38], N. Hod[243], A.M. Hodges[236], M.C. Hodgkinson[210], B.H. Hodkinson[180], A. Hoecker[62], D.D. Hofer[156], J. Hofer[237], J. Hofner[150], M. Holzbock[62], L.B.A.H. Hommels[46], V. Homsak[180], B.P. Honan[151], J.J. Hong[99], T.M. Hong[183], B.H. Hooberman[236], W.H. Hopkins[7], M.C. Hoppesch[236], Y. Horii[161], M.E. Horstmann[160], S. Hou[219], M.R. Housenga[236], J. Howarth[87], J. Hoya[7], M. Hrabovsky[176], T. Hryn'ova[5], P.J. Hsu[96], S.-C. Hsu[205], T. Hsu[97], M. Hu[19], Q. Hu[90], S. Huang[46], X. Huang[15,164], Y. Huang[193], Y. Huang[163], Y. Huang[15], Z. Huang[97], Z. Hubacek[192], F. Huegging[31], T.B. Huffman[180], M. Hufnagel Maranha De Faria[125], C.A. Hugli[75], M. Huhtinen[62], S.K. Huiberts[18], R. Hulsken[154], C.E. Hultquist[19], D.L. Humphreys[153], N. Huseynov[13], J. Huston[157], J. Huth[89], L. Huth[75], R. Hyneman[8], G. Iacobucci[83], G. Iakovidis[43], L. Iconomidou-Fayard[97], J.P. Iddon[62], P. Iengo[107,108], R. Iguchi[226], Y. Iiyama[226], T. Iizawa[226], Y. Ikegami[130], D. Iliadis[225], N. Ilic[228], H. Imam[56], G. Inacio Goncalves[128], S.A. Infante Cabanas[199], T. Ingebretsen Carlson[73,74], J.M. Inglis[144], G. Introzzi[109,110], M. Iodice[117], V. Ippolito[113,114], R.K. Irwin[142], M. Ishino[226], W. Islam[244], C. Issever[21], S. Istin[XLII,24], K. Itabashi[130], H. Ito[242], R. Iuppa[119,120], A. Ivina[243], V. Izzo[107], P. Jacka[192], P. Jackson[1], P. Jain[75], K. Jakobs[81], T. Jakoubek[243], J. Jamieson[87], W. Jang[226], S. Jankovych[193], M. Javurkova[153], P. Jawahar[151], L. Jeanty[177], J. Jejelava[XXXII,220], P. Jenni[VII,81], C.E. Jessiman[55], C. Jia[206], H. Jia[238], J. Jia[216], X. Jia[160,164], Z. Jia[162], C. Jiang[79], Q. Jiang[94], S. Jiggins[75], M. Jimenez Ortega[237], J. Jimenez Pena[14], S. Jin[162], A. Jinaru[35], O. Jinnouchi[204], P. Johansson[210], K.A. Johns[8], J.W. Johnson[196], F.A. Jolly[75], D.M. Jones[217], E. Jones[75], K.S. Jones[9], P. Jones[46], R.W.L. Jones[141], T.J. Jones[142], H.L. Joos[82], R. Joshi[173], J. Jovicevic[17], X. Ju[19], J.J. Junggeburth[62], T. Junkermann[91], A. Juste Rozas[XXV,14], M.K. Juzek[136], S. Kabana[202], A. Kaczmarska[136], S.A. Kadir[214], M. Kado[160], H. Kagan[173], M. Kagan[214], A. Kahn[182], C. Kahra[150], T. Kaji[226], E. Kajomovitz[223], N. Kakati[243], N. Kakoty[14], I. Kalaitzidou[81], S. Kandel[9], N. Kanellos[11], N.J. Kang[196], D. Kar[I,54], E. Karentzos[31], K. Karki[9], O. Karkout[167], S.N. Karpov[64], Z.M. Karpova[64], V. Kartvelishvili[141], A.N. Karyukhin[63], E. Kasimi[225], J. Katzy[75], S. Kaur[55], K. Kawade[211], M.P. Kawale[174], C. Kawamoto[137], T. Kawamoto[90], E.F. Kay[62], F.I. Kaya[232], S. Kazakos[157], K. Kazakova[152], V.F. Kazanin[63], J.M. Keaveney[47], R. Keeler[239], G.V. Kehris[89], J.S. Keller[55], J.M. Kelly[239], J.J. Kempster[217], O. Kepka[191], J. Kerr[230], B.P. Kerridge[194], B.P. Kerševan[143], L. Keszeghova[41], R.A. Khan[183], A. Khanov[175], A.G. Kharlamov[63], T. Kharlamova[63], E.E. Khoda[205], M. Kholodenko[184], T.J. Khoo[21], G. Khoriauli[240], Y. Khoulaki[56], J. Khubua[I,221], Y.A.R. Khwaira[181], B. Kibirige[54], D. Kim[7], D.W. Kim[73,74], Y.K. Kim[65], N. Kimura[146], M.K. Kingston[82], A. Kirchhoff[82], C. Kirfel[31], F. Kirfel[31], J. Kirk[194], A.E. Kiryunin[160], S. Kita[231], O. Kivernyk[31], M. Klassen[232], C. Klein[55], L. Klein[240], M.H. Klein[71], S.B. Klein[83], U. Klein[142], A. Klimentov[43], T. Klioutchnikova[62], P. Kluit[167], S. Kluth[160], E. Kneringer[121], T.M. Knight[228], A. Knue[76], M. Kobel[77], D. Kobylianskii[243], S.F. Koch[180], M. Kocian[214], P. Kodyš[193], D.M. Koeck[177], T. Koffas[55], O. Kolay[77], I. Koletsou[5], T. Komarek[136], K. Köneke[82], A.X.Y. Kong[1], T. Kono[172], N. Konstantinidis[146], P. Kontaxakis[83], B. Konya[148], R. Kopeliansky[67], S. Koperny[134], K. Korcyl[136], K. Kordas[V,225], A. Korn[146], S. Korn[82], I. Korolkov[14], N. Korotkova[63], B. Kortman[167], O. Kortner[160], S. Kortner[160], W.H. Kostecka[168], M. Kostov[41], V.V. Kostyukhin[212], A. Kotsokechagia[62], A. Kotwal[78], A. Koulouris[62], A. Kourkoumeli-Charalampidi[109,110], C. Kourkoumelis[10], E. Kourlitis[160], O. Kovanda[177], R. Kowalewski[239], W. Kozanecki[177], A.S. Kozhin[63], V.A. Kramarenko[63], G. Kramberger[143], P. Kramer[31], M.W. Krasny[181], A. Krasznahorkay[153], A.C. Kraus[168], J.W. Kraus[245], J.A. Kremer[75], N.B. Krengel[212], T. Kresse[77], L. Kretschmann[245], J. Kretzschmar[142], P. Krieger[228], K. Krizka[23], K. Kroeninger[76], H. Kroha[160], J. Kroll[191], J. Kroll[182], K.S. Krowpman[157], U. Kruchonak[64], H. Krüger[31], N. Krumnack[123], M.C. Kruse[78], O. Kuchinskaia[64], S. Kuday[3], S. Kuehn[62], R. Kuesters[81], T. Kuhl[75], V. Kukhtin[64], Y. Kulchitsky[64], S. Kuleshov[200,198], J. Kull[1], E.V. Kumar[159], M. Kumar[54], N. Kumari[75], P. Kumari[230], A. Kupco[191], A. Kupich[63], O. Kuprash[81], H. Kurashige[133], L.L. Kurchaninov[229], O. Kurdysh[5], Y.A. Kurochkin[63], A. Kurova[63], M. Kuze[204], A.K. Kvam[153], J. Kvita[176], N.G. Kyriacou[205], C. Lacasta[237], F. Lacava[113,114], H. Lacker[21], D. Lacour[181], N.N. Lad[146], E. Ladygin[64], A. Lafarge[66], B. Laforge[181], T. Lagouri[246], F.Z. Lahbabi[56], S. Lai[82,62], W.S. Lai[146], J.E. Lambert[239], S. Lammers[99], W. Lampl[8], C. Lampoudis[V,225], G. Lamprinoudis[150], A.N. Lancaster[168], E. Lançon[43], U. Landgraf[81], M.P.J. Landon[144], V.S. Lang[81], O.K.B. Langrekken[179], A.J. Lankford[233], F. Lanni[62], K. Lantzsch[31], A. Lanza[109], M. Lanzac Berrocal[237], J.F. Laporte[195], T. Lari[105], D. Larsen[18], L. Larson[12], F. Lasagni Manghi[30], M. Lassnig[62], S.D. Lawlor[210], R. Lazaridou[233], M. Lazzaroni[105,106], E.T.T. Le[233], H.D.M. Le[157], E.M. Le Boulicaut[246], L.T. Le Pottier[19], B. Leban[30,29], F. Ledroit-Guillon[88], T.F. Lee[230], L.L. Leeuw[49], M. Lefebvre[239], C. Leggett[19], G. Lehmann Miotto[62], M. Leigh[83], W.A. Leight[153], W. Leinonen[166], A. Leisos[XXII,225], M.A.L. Leite[127], C.E. Leitgeb[21], R. Leitner[193], K.J.C. Leney[71], T. Lenz[31], S. Leone[111], C. Leonidopoulos[79], A. Leopold[215], J. LePage-Bourbonnais[55], R. Les[157], C.G. Lester[46], M. Levchenko[63], J. Levêque[5], L.J. Levinson[243], G. Levrini[30,29], M.P. Lewicki[136], C. Lewis[205], D.J. Lewis[5], L. Lewitt[210], A. Li[43], B. Li[206], C. Li[156], C-Q. Li[160], H. Li[206], H. Li[151], H. Li[16], H. Li[90], H. Li[206], J. Li[208], K. Li[15], L. Li[208], R. Li[246], S. Li[15,164], S. Li[209,208], T. Li[6], X. Li[154], Y. Li[15], Z. Li[226], Z. Li[15,164], Z. Li[90], S. Liang[15,164], Z. Liang[15], M. Liberatore[195], B. Liberti[115], G.B. Libotte[128], K. Lie[95], J. Lieber Marin[129], H. Lien[99], H. Lin[156], S.F. Lin[216], L. Linden[159], R.E. Lindley[8], J.H. Lindon[62], J. Ling[89], E. Lipeles[182], A. Lipniacka[18], A. Lister[238], J.D. Little[99], B. Liu[15], B.X. Liu[163], D. Liu[209,208], D. Liu[196], E.H.L. Liu[23], J.K.K. Liu[171], K. Liu[209], K. Liu[209,208],

M. Liu[90], M.Y. Liu[90], P. Liu[15], Q. Liu[209,205,208], S. Liu[216], X. Liu[90], X. Liu[206], Y. Liu[163,164], Y. Liu[236], Y.L. Liu[206], Y.W. Liu[90], Z. Liu[XII,97], S.L. Lloyd[144], E.M. Lobodzinska[75], P. Loch[8], E. Lodhi[228], K. Lohwasser[210], E. Loiacono[75], J.D. Lomas[23], J.D. Long[67], I. Longarini[233], R. Longo[236], A. Lopez Solis[14], N.A. Lopez-canelas[8], N. Lorenzo Martinez[5], A.M. Lory[159], M. Losada[169], G. Löschcke Centeno[5], X. Lou[73,74], X. Lou[15,164], A. Lounis[97], P.A. Love[141], M. Lu[97], S. Lu[182], Y.J. Lu[219], H.J. Lubatti[205], C. Luci[113,114], F.L. Lucio Alves[162], F. Luehring[99], B.S. Lunday[182], O. Lundberg[215], J. Lunde[62], N.A. Luongo[7], M.S. Lutz[62], A.B. Lux[32], D. Lynn[43], R. Lysak[191], V. Lysenko[192], E. Lytken[148], V. Lyubushkin[64], T. Lyubushkina[64], M.M. Lyukova[216], H. Ma[43], K. Ma[90], L.L. Ma[206], W. Ma[90], Y. Ma[175], J.C. MacDonald[150], P.C. Machado De Abreu Farias[129], D. Macina[62], R. Madar[66], T. Madula[146], J. Maeda[133], T. Maeno[43], P.T. Mafa[XI,49], H. Maguire[210], M. Maheshwari[46], V. Maiboroda[97], A. Maio[184,185,187], K. Maj[134], O. Majersky[75], S. Majewski[177], R. Makhmanazarov[63], N. Makovec[97], V. Maksimovic[17], B. Malaescu[181], J. Malamant[179], Pa. Malecki[136], V.P. Maleev[63], F. Malek[XVI,88], M. Mali[143], D. Malito[145], U. Mallik[I,122], A. Maloizel[6], S. Maltezos[11], A. Malvezzi Lopes[128], S. Malyukov[64], J. Mamuzic[143], G. Mancini[80], M.N. Mancini[33], G. Manco[109,110], J.P. Mandalia[144], S.S. Mandarry[217], I. Mandić[143], L. Manhaes de Andrade Filho[125], I.M. Maniatis[243], J. Manjarres Ramos[139], D.C. Mankad[243], A. Mann[159], T. Manoussos[62], M.N. Mantinan[65], S. Manzoni[62], L. Mao[208], X. Mapekula[49], A. Marantis[225], R.R. Marcelo Gregorio[144], G. Marchiori[6], C. Marcon[105], E. Maricic[17], M. Marinescu[75], S. Marium[75], M. Marjanovic[174], A. Markhoos[81], M. Markovitch[97], M.K. Maroun[153], M.C. Marr[213], G.T. Marsden[151], E.J. Marshall[141], Z. Marshall[19], S. Marti-Garcia[237], J. Martin[146], T.A. Martin[194], V.J. Martin[79], B. Martin dit Latour[18], L. Martinelli[113,114], M. Martinez[XXV,14], P. Martinez Agullo[237], V.I. Martinez Outschoorn[153], P. Martinez Suarez[62], S. Martin-Haugh[194], G. Martinovicova[193], V.S. Martoiu[35], A.C. Martyniuk[146], A. Marzin[62], D. Mascione[119,120], L. Masetti[150], J. Masik[151], A.L. Maslennikov[64], S.L. Mason[67], P. Massarotti[107,108], P. Mastrandrea[111,112], A. Mastroberardino[70,69], T. Masubuchi[178], T.T. Mathew[177], J. Matousek[193], D.M. Mattern[76], J. Maurer[35], T. Maurin[87], A.J. Maury[97], B. Maček[143], C. Mavungu Tsava[152], D.A. Maximov[63], A.E. May[151], E. Mayer[66], R. Mazini[54], I. Maznas[168], S.M. Mazza[196], E. Mazzeo[62], J.P. Mc Gowan[239], S.P. Mc Kee[156], C.A. Mc Lean[7], C.C. McCracken[238], E.F. McDonald[155], A.E. McDougall[167], L.F. Mcelhinney[141], J.A. Mcfayden[217], R.P. McGovern[182], R.P. Mckenzie[54], T.C. Mclachlan[75], D.J. Mclaughlin[146], S.J. McMahon[194], C.M. Mcpartland[142], R.A. McPherson[XXIX,239], S. Mehlhase[159], A. Mehta[142], D. Melini[237], B.R. Mellado Garcia[54], A.H. Melo[82], F. Meloni[75], A.M. Mendes Jacques Da Costa[151], L. Meng[141], S. Menke[160], M. Mentink[62], E. Meoni[70,69], G. Mercado[168], S. Merianos[225], C. Merlassino[100,102], C. Meroni[105,106], J. Metcalfe[7], A.S. Mete[7], E. Meuser[150], C. Meyer[99], J-P. Meyer[195], Y. Miao[162], R.P. Middleton[194], M. Mihovilovic[97], L. Mijović[79], G. Mikenberg[243], M. Mikestikova[191], M. Mikuž[143], H. Mildner[150], A. Milic[62], D.W. Miller[65], E.H. Miller[214], A. Milov[243], D.A. Milstead[73,74], T. Min[162], A.A. Minaenko[63], I.A. Minashvili[221], A.I. Mincer[171], B. Mindur[134], M. Mineev[64], Y. Mino[137], L.M. Mir[14], M. Miralles Lopez[87], M. Mironova[19], M. Missio[66], A. Mitra[241], V.A. Mitsou[237], Y. Mitsumori[161], O. Miu[228], P.S. Miyagawa[144], T. Mkrtchyan[62], M. Mlinarevic[146], T. Mlinarevic[146], M. Mlynarikova[193], L. Mlynarska[134], C. Mo[208], S. Mobius[22], M.H. Mohamed Farook[165], S. Mohapatra[67], M.F. Mohd Soberi[79], S. Mohiuddin[175], G. Mokgatitswane[54], L. Moleri[243], U. Molinatti[180], L.G. Mollier[22], B. Mondal[191], S. Mondal[192], K. Mönig[75], E. Monnier[152], L. Monsonis Romero[237], J. Montejo Berlingen[14], A. Montella[73,74], M. Montella[173], F. Montereali[117,118], F. Monticelli[140], S. Monzani[100,102], A. Morancho Tarda[68], N. Morange[97], A.L. Moreira De Carvalho[75], M. Moreno Llácer[237], C. Moreno Martinez[83], J.M. Moreno Perez[28], P. Morettini[85], S. Morgenstern[62], M. Morii[89], M. Morinaga[226], M. Moritsu[138], F. Morodei[113,114], P. Moschovakos[62], B. Moser[81], M. Mosidze[221], T. Moskalets[71], P. Moskvitina[166], J. Moss[45], P. Moszkowicz[134], T. Motta Quirino[128], A. Moussa[59], Y. Moyal[243], H. Moyano Gomez[14], E.J.W. Moyse[153], T.G. Mroz[136], O. Mtintsilana[54], S. Muanza[152], M. Mucha[31], J. Mueller[183], G.A. Mullier[235], A.J. Mullin[46], J.J. Mullin[78], A.C. Mullins[71], A.E. Mulski[89], D.P. Mungo[228], D. Munoz Perez[237], F.J. Munoz Sanchez[151], W.J. Murray[241,194], M. Muškinja[143], C. Mwewa[75], A.G. Myagkov[II,63], A.J. Myers[9], G. Myers[156], M. Myska[192], B.P. Nachman[214], K. Nagai[180], K. Nagano[130], R. Nagasaka[226], J.L. Nagle[XXXIX,43], E. Nagy[152], A.M. Nairz[62], Y. Nakahama[130], K. Nakamura[130], K. Nakkalil[6], A. Nandi[92], H. Nanjo[178], E.A. Narayanan[71], Y. Narukawa[226], I. Naryshkin[63], L. Nasella[105,106], S. Nasri[170], C. Nass[31], G. Navarro[27], A. Nayaz[21], P.Y. Nechaeva[63], S. Nechaeva[30,29], F. Nechansky[191], L. Nedic[180], T.J. Neep[23], A. Negri[109,110], M. Negrini[30], C. Nellist[167], C. Nelson[154], K. Nelson[156], S. Nemecek[191], M. Nessi[VIII,62], M.S. Neubauer[236], J. Newell[142], P.R. Newman[23], Y.W.Y. Ng[236], B. Ngair[169], H.D.N. Nguyen[158], J.D. Nichols[174], R.B. Nickerson[180], R. Nicolaidou[195], J. Nielsen[196], M. Niemeyer[82], J. Niermann[62], N. Nikiforou[62], V. Nikolaenko[II,63], I. Nikolic-Audit[181], P. Nilsson[43], I. Ninca[75], G. Ninio[224], A. Nisati[113], R. Nisius[160], N. Nitika[243], J-E. Nitschke[77], E.K. Nkadimeng[48], T. Nobe[226], D. Noll[19], T. Nommensen[218], M.B. Norfolk[210], B.J. Norman[55], L.C. Nosler[19], M. Noury[56], J. Novak[143], T. Novak[143], R. Novotny[192], L. Nozka[176], K. Ntekas[233], D. Ntounis[214], N.M.J. Nunes De Moura Junior[126], J. Ocariz[181], I. Ochoa[184], S. Oerdek[75], J.T. Offermann[65], A. Ogrodnik[136], A. Oh[151], C.C. Ohm[215], H. Oide[130], M.L. Ojeda[62], Y. Okumura[226], L.F. Oleiro Seabra[184], I. Oleksiyuk[83], G. Oliveira Correa[14], D. Oliveira Damazio[43], J.L. Oliver[1], R. Omar[99], Ö.O. Öncel[81], A.P. O'Neill[22], A. Onofre[VI,184,188], P.U.E. Onyisi[12], M.J. Oreglia[65], D. Orestano[117,118], R. Orlandini[117,118], R.S. Orr[228], L.M. Osojnak[67], Y. Osumi[161], G. Otero y Garzón[44], H. Otono[138], M. Ouchrif[59], F. Ould-Saada[179], T. Ovsiannikova[205], M. Owen[87], R.E. Owen[194], V.E. Ozcan[24], F. Ozturk[136], N. Ozturk[9], S. Ozturk[124], H.A. Pacey[180], K. Pachal[229], A. Pacheco Pages[14], C. Padilla Aranda[14], G. Padovano[113,114], S. Pagan Griso[19], G. Palacino[99], A. Palazzo[103,104], J. Pampel[31], J. Pan[246], T. Pan[93], D.K. Panchal[12], C.E. Pandini[88], J.G. Panduro Vazquez[194], H.D. Pandya[1], H. Pang[195], P. Pani[75], G. Panizzo[100,102], L. Panwar[181], L. Paolozzi[83], S. Parajuli[236], A. Paramonov[7], C. Paraskevopoulos[80], D. Paredes Hernandez[94], A. Pareti[109,110], K.R. Park[67], T.H. Park[160], F. Parodi[85,84], J.A. Parsons[67], U. Parzefall[81], B. Pascual Dias[66], L. Pascual Dominguez[149], E. Pasqualucci[113], S. Passaggio[85], F. Pastore[145], P. Patel[136], U.M. Patel[78], J.R. Pater[151], T. Pauly[62], F. Pauwels[193], C.I. Pazos[232], M. Pedersen[179], R. Pedro[184], S.V. Peleganchuk[63], O. Penc[191], S. Peng[16], G.D. Penn[246], K.E. Penski[159], M. Penzin[63], B.S. Peralva[128], A.P. Pereira Peixoto[205], L. Pereira Sanchez[214], D.V. Perepelitsa[XXXIX,43], G. Perera[153], E. Perez Codina[62], M. Perganti[11], H. Pernegger[62], S. Perrella[113,114], K. Peters[75], R.F.Y. Peters[151], B.A. Petersen[62], T.C. Petersen[68], E. Petit[152], V. Petousis[192], A.R. Petri[105,106], C. Petridou[V,225], T. Petru[193], A. Petrukhin[212], M. Pettee[19], A. Petukhov[124], K. Petukhova[62], R. Pezoa[203], L. Pezzotti[30,29], G. Pezzullo[246], L. Pfaffenbichler[62], A.J. Pfleger[121], T.M. Pham[244], T. Pham[155], P.W. Phillips[194], G. Piacquadio[216], E. Pianori[19], F. Piazza[177], R. Piegaia[44], D. Pietreanu[35], A.D. Pilkington[151], M. Pinamonti[100,102], J.L. Pinfold[2], B.C. Pinheiro Pereira[184], J. Pinol Bel[14], A.E. Pinto Pinoargote[181], L. Pintucci[100,102], K.M. Piper[217], A. Pirttikoski[83], D.A. Pizzi[55], L. Pizzimento[94], A. Plebani[46], M.-A. Pleier[43], V. Pleskot[193], E. Plotnikova[64], G. Poddar[144], R. Poettgen[148], L. Poggioli[181], S. Polacek[193], G. Polesello[109], A. Poley[213], A. Polini[30], C.S. Pollard[241], Z.B. Pollock[173], E. Pompa Pacchi[174], N.I. Pond[146], D. Ponomarenko[99], L. Pontecorvo[62], S. Popa[34], G.A. Popeneciu[37], A. Poreba[62], D.M. Portillo Quintero[229], S. Pospisil[192], M.A. Postill[210], P. Postolache[36], K. Potamianos[241], P.A. Potepa[134], I.N. Potrap[64], C.J. Potter[46], H. Potti[218], J. Poveda[237], M.E. Pozo Astigarraga[62], R. Pozzi[62], A. Prades Ibanez[115,116], S.R. Pradhan[210], J. Pretel[239], D. Price[151], M. Primavera[103], L. Primomo[100,102], M.A. Principe Martin[149], R. Privara[176], T. Procter[135], M.L. Proffitt[205], N. Proklova[182], K. Prokofiev[95], G. Proto[160], J. Proudfoot[7], M. Przybycien[134], W.W. Przygoda[135], A. Psallidas[72], J.E. Puddefoot[210], D. Pudzha[80], H.I. Purnell[1], D. Pyatiizbyantseva[166], J. Qian[156], R. Qian[157], D. Qichen[180], Y. Qin[14], T. Qiu[79], A. Quadt[82], M. Queitsch-Maitland[151], G. Quetant[83], R.P. Quinn[238], G. Rabanal Bolanos[89], D. Rafanoharana[160], F. Raffaeli[115,116], F. Ragusa[105,106], J.L. Rainbolt[65], S. Rajagopalan[43], E. Ramakoti[64], L. Rambelli[85,84], I.A. Ramirez-Berend[55], K. Ran[75,164], D.S. Rankin[182], N.P. Rapheeha[54], H. Rasheed[35], D.F. Rassloff[91], A. Rastogi[19], S. Rave[150], S. Ravera[85,84], B. Ravina[62], I. Ravinovich[243], M. Raymond[62], A.L. Read[179], N.P. Readioff[210], D.M. Rebuzzi[109,110], A.S. Reed[87], K. Reeves[33], J.A. Reidelsturz[245], D. Reikher[62], A. Rej[76], C. Rembser[62], H. Ren[90], M. Renda[35], F. Renner[75], A.G. Rennie[87], M. Repik[83], A.L. Rescia[85,84], S. Resconi[105], M. Ressegotti[85], S. Rettie[167], W.F. Rettie[55], M.M. Revering[46], E. Reynolds[19], O.L. Rezanova[64], P. Reznicek[193], H. Riani[59], N. Ribaric[78], B. Ricci[100,102], E. Ricci[119,120], R. Richter[160], S. Richter[73,74], E. Richter-Was[135], M. Ridel[181], S. Ridouani[59], P. Rieck[171], P. Riedler[62], E.M. Riefel[73,74], J.O. Rieger[167], M. Rijssenbeek[216], M. Rimoldi[62], L. Rinaldi[30,29], P. Rincke[235,82], G. Ripellino[235], I. Riu[14], J.C. Rivera Vergara[239], F. Rizatdinova[175], E. Rizvi[144], B.R. Roberts[19], S.S. Roberts[196], D. Robinson[46], M. Robles Manzano[150], A. Robson[87], A. Rocchi[115,116], C. Roda[111,112], S. Rodriguez Bosca[62], Y. Rodriguez Garcia[27], A.M. Rodríguez Vera[168], S. Roe[62], J.T. Roemer[62], O. Røhne[179], R.A. Rojas[62], C.P.A. Roland[181], A. Romaniouk[121], E. Romano[109,110], M. Romano[30], A.C. Romero Hernandez[236], N. Rompotis[142], L. Roos[181], S. Rosati[113], B.J. Rosser[65], E. Rossi[180], E. Rossi[107,108], L.P. Rossi[89], L. Rossini[81], R. Rosten[173], M. Rotaru[35], R. Roth[62], B. Rottler[81], D. Rousseau[97], D. Rousso[75], S. Roy-Garand[228], A. Rozanov[152], Z.M.A. Rozario[87], Y. Rozen[223], A. Rubio Jimenez[237], V.H. Ruelas Rivera[21], T.A. Ruggeri[1], A. Ruggiero[180], A. Ruiz-Martinez[237], A. Rummler[62], Z. Rurikova[81], N.A. Rusakovich[64], S. Ruscelli[76], H.L. Russell[239], G. Russo[113,114], J.P. Rutherfoord[8], S. Rutherford Colmenares[46], M. Rybar[193], P. Rybczynski[134], A. Ryzhov[71], J.A. Sabater Iglesias[83], H.F-W. Sadrozinski[196], F. Safai Tehrani[113], S. Saha[1], M. Sahinsoy[124], B. Sahoo[243], A. Saibel[237], B.T. Saifuddin[174], M. Saimpert[195], G.T. Saito[127], M. Saito[226], T. Saito[226], A. Sala[105,106], A. Salnikov[214], J. Salt[237], A. Salvador Salas[224], F. Salvatore[217], A. Salzburger[62], D. Sammel[81], E. Sampson[141], D. Sampsonidis[V,225], D. Sampsonidou[177], M.A.A. Samy[87], J. Sánchez[237], V. Sanchez Sebastian[237], H. Sandaker[179], C.O. Sander[75], J.A. Sandesara[244], M. Sandhoff[245], C. Sandoval[28], L. Sanfilippo[91], D.P.C. Sankey[194], T. Sano[137], A. Sansoni[80], M. Santana Queiroz[20], L. Santi[62], C. Santoni[66], H. Santos[184,185], A. Santra[243], E. Sanzani[30,29], K.A. Saoucha[132], J.G. Saraiva[184,187], J. Sardain[8], O. Sasaki[130], K. Sato[231], C. Sauer[62], E. Sauvan[5], P. Savard[XXXVI,228], R. Sawada[226], C. Sawyer[194], L. Sawyer[147], C. Sbarra[30], A. Sbrizzi[30,29], T. Scanlon[146], J. Schaarschmidt[205], U. Schäfer[150], A.C. Schaffer[97,71], D. Schaile[159], R.D. Schamberger[216], C. Scharf[21], M.M. Schefer[22], V.A. Schegelsky[63], D. Scheirich[193], M. Schernau[202], C. Scheulen[83], C. Schiavi[85,84], M. Schioppa[70,69], B. Schlag[214], S. Schlenker[62], J. Schmeing[245], E. Schmidt[160], M.A. Schmidt[245], K. Schmieden[31], C. Schmitt[150], N. Schmitt[150], S. Schmitt[75], N.A. Schneider[159], L. Schoeffel[195], A. Schoening[92], P.G. Scholer[55], E. Schopf[212], M. Schott[31], S. Schramm[83], T. Schroer[83], H-C. Schultz-Coulon[91], M. Schumacher[81], B.A. Schumm[196], Ph. Schune[195], H.R. Schwartz[8], A. Schwartzman[214], T.A. Schwarz[156], Ph. Schwemling[195], R. Schwienhorst[157], F.G. Sciacca[22], A. Sciandra[43], G. Sciolla[33], F. Scuri[111], C.D. Sebastiani[62], K. Sedlaczek[168], S.C. Seidel[165], A. Seiden[196], B.D. Seidlitz[67], C. Seitz[75], J.M. Seixas[126], G. Sekhniaidze[107], L. Selem[88], N. Semprini-Cesari[30,29], A. Semushin[247], D. Sengupta[83], V. Senthilkumar[237], L. Serin[97], M. Sessa[107,108], H. Severini[174], F. Sforza[85,84], A. Sfyrla[83], Q. Sha[15], E. Shabalina[82], H. Shaddix[168], A.H. Shah[46], R. Shaheen[215], J.D. Shahinian[182], M. Shamim[62], L.Y. Shan[15], M. Shapiro[19], A. Sharma[62], A.S. Sharma[238], P. Sharma[43], P.B. Shatalov[63], K. Shaw[217], S.M. Shaw[151], Q. Shen[15], D.J. Sheppard[213], P. Sherwood[146], L. Shi[146], X. Shi[15], S. Shimizu[130], C.O. Shimmin[246], I.P.J. Shipsey[I,180], S. Shirabe[138], M. Shiyakova[XXVII,64], M.J. Shochet[65], D.R. Shope[179], B. Shrestha[174], S. Shrestha[XLI,173], I. Shreyber[64], M.J. Shroff[239], P. Sicho[191], A.M. Sickles[236], E. Sideras Haddad[54,234], A.C. Sidley[167], A. Sidoti[30], F. Siegert[77], Dj. Sijacki[17], F. Sili[140], J.M. Silva[79], I. Silva Ferreira[126], M.V. Silva Oliveira[43], S.B. Silverstein[73], S. Simion[97], R. Simoniello[62], E.L. Simpson[151], H. Simpson[217], L.R. Simpson[7], S. Simsek[124], S. Sindhu[82], P. Sinervo[228], S.N. Singh[33], S. Singh[43], S. Sinha[75], S. Sinha[151], M. Sioli[30,29], K. Sioulas[10], I. Siral[62], E. Sitnikova[75], J. Sjölin[73,74], A. Skaf[82], E. Skorda[23], P. Skubic[174], M. Slawinska[136], I. Slazyk[18], I. Sliusar[179], V. Smakhtin[243], B.H. Smart[194], S.Yu. Smirnov[198], Y. Smirnov[124], L.N. Smirnova[II,63], O. Smirnova[148], A.C. Smith[67], D.R. Smith[233], J.L. Smith[151], M.B. Smith[55], R. Smith[214], H. Smitmanns[150], M. Smizanska[141], K. Smolek[192], P. Smolyanskiy[192], A.A. Snesarev[64], H.L. Snoek[167], S. Snyder[43], R. Sobie[XXIX,239], A. Soffer[224], C.A. Solans Sanchez[62], E.Yu. Soldatov[64], U. Soldevila[237], A.A. Solodkov[54], S. Solomon[33], A. Soloshenko[64], K. Solovieva[81], O.V. Solovyanov[66], P. Sommer[77], A. Sonay[14], A. Sopczak[192], A.L. Sopio[79], F. Sopkova[42], J.D. Sorenson[165], I.R. Sotarriva Alvarez[204], V. Sothilingam[91], O.J. Soto Sandoval[199,198], S. Sottocornola[99], R. Soualah[131], Z. Soumaimi[60], D. South[75], N. Soybelman[243], S. Spagnolo[103,104], M. Spalla[160], D. Sperlich[81], B. Spisso[107,108], D.P. Spiteri[87], L. Splendori[152], M. Spousta[193], E.J. Staats[55], R. Stamen[91], E. Stanecka[136], W. Stanek-Maslouska[75], M.V. Stange[77], B. Stanislaus[19], M.M. Stanitzki[75], B. Stapf[75], E.A. Starchenko[63], G.H. Stark[196], J. Stark[139], P. Staroba[191], P. Starovoitov[132], R. Staszewski[136], C. Stauch[159], G. Stavropoulos[72], A. Stefl[62], A. Stein[150], P. Steinberg[43], B. Stelzer[213,229], H.J. Stelzer[183], O. Stelzer[229], H. Stenzel[86], T.J. Stevenson[217], G.A. Stewart[62], J.R. Stewart[175], G. Stoicea[35], M. Stolarski[184], S. Stonjek[160], A. Straessner[77], J. Strandberg[215], S. Strandberg[73,74], M. Stratmann[245], M. Strauss[174], T. Strebler[152], P. Strizenec[42], R. Ströhmer[240], D.M. Strom[177], R. Stroynowski[71], A. Strubig[73,74], S.A. Stucci[43], B. Stugu[18], J. Stupak[174], N.A. Styles[75], D. Su[214], S. Su[90], X. Su[90], D. Suchy[41], A.D. Sudhakar Ponnu[82], K. Sugizaki[182], V.V. Sulin[63], D.M.S. Sultan[180], L. Sultanaliyeva[31], S. Sultansoy[4], S. Sun[244], W. Sun[15], N. Sur[148], M.R. Sutton[217], M. Svatos[191], P.N. Swallow[46], M. Swiatlowski[229], T. Swirski[240], A. Swoboda[62], I. Sykora[41], M. Sykora[193], T. Sykora[193], D. Ta[150], K. Tackmann[XXVI,75], A. Taffard[233], R. Tafirout[229], Y. Takubo[130], M. Talby[152], A.A. Talyshev[63], K.C. Tam[94], N.M. Tamir[224], A. Tanaka[226], J. Tanaka[226], R. Tanaka[97], M. Tanasini[216], Z. Tao[238], S. Tapia Araya[203], S. Tapprogge[150], A. Tarek Abouelfadl Mohamed[62], S. Tarem[223], K. Tariq[15], G. Tarna[62], G.F. Tartarelli[105], M.J. Tartarin[139], P. Tas[193], M. Tasevsky[191], E. Tassi[70,69], A.C. Tate[236], Y. Tayalati[XXVIII,60], G.N. Taylor[155], W. Taylor[230], R.J. Taylor Vara[237], A.S. Tegetmeier[139], P. Teixeira-Dias[145], J.J. Teoh[228], K. Terashi[226], J. Terron[149], S. Terzo[14], M. Testa[80], R.J. Teuscher[XXIX,228], A. Thaler[121], O. Theiner[83], T. Theveneaux-Pelzer[152], D.W. Thomas[145], J.P. Thomas[23], E.A. Thompson[19], P.D. Thompson[23], E. Thomson[182], R.E. Thornberry[71], C. Tian[90], Y. Tian[83], V. Tikhomirov[124], Yu.A. Tikhonov[64], S. Timoshenko[63], D. Timoshyn[193], E.X.L. Ting[1], P. Tipton[246], A. Tishelman-Charny[43], K. Todome[204], S. Todorova-Nova[193], L. Toffolin[100,102], M. Togawa[130], J. Tojo[138],

S. Tokár[41], O. Toldaiev[99], G. Tolkachev[152], M. Tomoto[130], L. Tompkins[XV,214], E. Torrence[177], H. Torres[139], D.I. Torres Arza[203], E. Torró Pastor[237], M. Toscani[44], C. Tosciri[65], M. Tost[12], D.R. Tovey[210], T. Trefzger[240], P.M. Tricarico[14], A. Tricoli[43], I.M. Trigger[229], S. Trincaz-Duvoid[181], D.A. Trischuk[33], A. Tropina[64], L. Truong[49], M. Trzebinski[136], A. Trzupek[136], F. Tsai[216], M. Tsai[156], A. Tsiamis[225], P.V. Tsiareshka[64], S. Tsigaridas[229], A. Tsirigotis[XXII,225], V. Tsiskaridze[220], E.G. Tskhadadze[220], Y. Tsujikawa[137], I.I. Tsukerman[63], V. Tsulaia[19], S. Tsuno[130], K. Tsuri[172], D. Tsybychev[216], Y. Tu[94], A. Tudorache[35], V. Tudorache[35], S.B. Tuncay[180], S. Turchikhin[85,84], I. Turk Cakir[3], R. Turra[105], T. Turtuvshin[XXX,64], P.M. Tuts[67], S. Tzamarias[V,225], Y. Uematsu[130], F. Ukegawa[231], P.A. Ulloa Poblete[199,198], E.N. Umaka[43], G. Unal[62], A. Undrus[43], G. Unel[233], J. Urban[42], P. Urrejola[201], G. Usai[9], R. Ushioda[227], M. Usman[158], F. Ustuner[79], Z. Uysal[124], V. Vacek[192], B. Vachon[154], T. Vafeiadis[62], A. Vaitkus[146], C. Valderanis[159], E. Valdes Santurio[73,74], M. Valente[62], S. Valentinetti[30,29], A. Valero[237], E. Valiente Moreno[237], A. Vallier[139], J.A. Valls Ferrer[237], D.R. Van Arneman[167], A. Van Der Graaf[76], H.Z. Van Der Schyf[54], P. Van Gemmeren[7], M. Van Rijnbach[62], S. Van Stroud[146], I. Van Vulpen[167], P. Vana[193], M. Vanadia[115,116], U.M. Vande Voorde[215], W. Vandelli[62], E.R. Vandewall[175], D. Vannicola[224], L. Vannoli[80], R. Vari[113], M. Varma[246], E.W. Varnes[8], C. Varni[168], D. Varouchas[97], L. Varriale[237], K.E. Varvell[218], M.E. Vasile[35], L. Vaslin[130], M.D. Vassilev[214], A. Vasyukov[64], L.M. Vaughan[175], R. Vavricka[193], T. Vazquez Schroeder[14], J. Veatch[45], V. Vecchio[151], M.J. Veen[153], I. Veliscek[43], I. Velkovska[143], L.M. Veloce[228], F. Veloso[184,186], S. Veneziano[113], A. Ventura[103,104], A. Verbytskyi[160], M. Verducci[111,112], C. Vergis[144], M. Verissimo De Araujo[126], W. Verkerke[167], J.C. Vermeulen[167], C. Vernieri[214], M. Vessella[233], M.C. Vetterli[XXXVI,213], A. Vgenopoulos[150], N. Viaux Maira[XXXIII,203], T. Vickey[210], O.E. Vickey Boeriu[210], G.H.A. Viehhauser[180], L. Vigani[92], M. Vigl[160], M. Villa[30,29], M. Villaplana Perez[237], E.M. Villhauer[65], E. Vilucchi[80], M. Vincent[237], M.G. Vincter[55], A. Visibile[167], A. Visive[167], C. Vittori[62], I. Vivarelli[30,29], M.I. Vivas Albornoz[75], E. Voevodina[160], F. Vogel[159], J.C. Voigt[77], P. Vokac[192], Yu. Volkotrub[135], L. Vomberg[31], E. Von Toerne[31], B. Vormwald[62], K. Vorobev[78], M. Vos[237], K. Voss[212], M. Vozak[62], L. Vozdecky[174], N. Vranjes[17], M. Vranjes Milosavljevic[17], M. Vreeswijk[167], N.K. Vu[209,208], R. Vuillermet[62], O. Vujinovic[150], I. Vukotic[65], I.K. Vyas[55], J.F. Wack[46], S. Wada[231], C. Wagner[214], J.M. Wagner[19], W. Wagner[245], S. Wahdan[245], H. Wahlberg[140], C.H. Waits[174], J. Walder[194], R. Walker[159], K. Walkingshaw Pass[87], W. Walkowiak[212], A. Wall[182], E.J. Wallin[148], T. Wamorkar[19], K. Wandall-Christensen[237], A. Wang[90], A.Z. Wang[196], C. Wang[150], C. Wang[12], H. Wang[19], J. Wang[95], P. Wang[151], P. Wang[146], R. Wang[89], R. Wang[7], S.M. Wang[219], S. Wang[15], T. Wang[166], T. Wang[90], W.T. Wang[180], W. Wang[15], X. Wang[236], X. Wang[208], X. Wang[75], Y. Wang[162], Y. Wang[90], Z. Wang[156], Z. Wang[209], Z. Wang[156], C. Wanotayaroj[130], A. Warburton[154], A.L. Warnerbring[212], S. Waterhouse[145], A.T. Watson[23], H. Watson[79], M.F. Watson[23], E. Watton[62], G. Watts[205], B.M. Waugh[146], J.M. Webb[81], C. Weber[43], H.A. Weber[21], M.S. Weber[22], S.M. Weber[91], C. Wei[90], Y. Wei[81], A.R. Weidberg[180], E.J. Weik[171], J. Weingarten[76], C. Weiser[81], C.J. Wells[75], T. Wenaus[43], T. Wengler[62], N.S. Wenke[160], N. Wermes[31], M. Wessels[91], A.M. Wharton[141], A.S. White[89], A. White[9], M.J. White[1], D. Whiteson[233], L. Wickremasinghe[178], W. Wiedenmann[244], M. Wielers[194], R. Wierda[215], C. Wiglesworth[68], H.G. Wilkens[62], J.J.H. Wilkinson[46], D.M. Williams[67], H.H. Williams[182], S. Williams[46], S. Willocq[153], B.J. Wilson[151], D.J. Wilson[151], P.J. Windischhofer[65], F.I. Winkel[44], F. Winklmeier[177], B.T. Winter[81], M. Wittgen[214], M. Wobisch[147], T. Wojtkowski[88], Z. Wolffs[167], J. Wollrath[62], M.W. Wolter[136], H. Wolters[184,186], M.C. Wong[196], E.L. Woodward[67], S.D. Worm[75], B.K. Wosiek[136], K.W. Woźniak[136], S. Wozniewski[82], K. Wraight[87], C. Wu[228], C. Wu[23], J. Wu[226], M. Wu[163], M. Wu[166], S.L. Wu[244], S. Wu[XXXVIII,15], X. Wu[90], Y.Q. Wu[228], Y. Wu[90], Z. Wu[5], Z. Wu[162], J. Wuerzinger[160], T.R. Wyatt[151], B.M. Wynne[79], S. Xella[68], L. Xia[162], M. Xie[90], A. Xiong[177], D. Xu[15], H. Xu[90], L. Xu[90], R. Xu[182], T. Xu[156], Y. Xu[205], Z. Xu[79], R. Xue[183], B. Yabsley[218], S. Yacoob[47], Y. Yamaguchi[130], E. Yamashita[226], H. Yamauchi[231], T. Yamazaki[19], Y. Yamazaki[133], S. Yan[87], Z. Yan[153], H.J. Yang[208,209], H.T. Yang[90], S. Yang[90], T. Yang[95], X. Yang[62], X. Yang[15], Y. Yang[226], Y. Yang[90], W-M. Yao[19], C.L. Yardley[217], J. Ye[15], S. Ye[43], X. Ye[90], Y. Yeh[146], I. Yeletskikh[64], B. Yeo[20], M.R. Yexley[146], T.P. Yildirim[180], K. Yorita[242], C.J.S. Young[62], C. Young[214], N.D. Young[177], Y. Yu[90], J. Yuan[XXXVIII,15,164], M. Yuan[156], R. Yuan[209,208], L. Yue[146], M. Zaazoua[90], B. Zabinski[136], I. Zahir[56], 57a, A. Zaio[85], Z.K. Zak[136], T. Zakareishvili[237], S. Zambito[83], J.A. Zamora Saa[200], J. Zang[226], R. Zanzottera[105,106], O. Zaplatilek[192], C. Zeitnitz[245], H. Zeng[15], J.C. Zeng[236], D.T. Zenger Jr[33], O. Zenin[63], T. Ženiš[41], S. Zenz[144], D. Zerwas[97], M. Zhai[15,164], D.F. Zhang[210], G. Zhang[XXXVIII,15], J. Zhang[206], J. Zhang[7], K. Zhang[15,164], L. Zhang[90], L. Zhang[162], P. Zhang[15,164], R. Zhang[162], S. Zhang[139], T. Zhang[226], Y. Zhang[205], Y. Zhang[146], Y. Zhang[90], Y. Zhang[162], Z. Zhang[19], Z. Zhang[206], Z. Zhang[97], H. Zhao[205], T. Zhao[206], Y. Zhao[55], Z. Zhao[90], Z. Zhao[90], A. Zhemchugov[64], J. Zheng[162], K. Zheng[236], X. Zheng[90], Z. Zheng[214], D. Zhong[236], B. Zhou[156], H. Zhou[8], N. Zhou[208], Y. Zhou[16], Y. Zhou[162], Y. Zhou[8], C.G. Zhu[206], J. Zhu[156], X. Zhu[209], Y. Zhu[208], Y. Zhu[90], X. Zhuang[15], K. Zhukov[99], N.I. Zimine[64], J. Zinsser[92], M. Ziolkowski[212], L. Živković[17], A. Zoccoli[30,29], K. Zoch[89], A. Zografos[62], T.G. Zorbas[210], O. Zormpa[72], L. Zwalinski[62]

Affiliation Notes

[I] Deceased
[II] Also at Affiliated with an institute formerly covered by a cooperation agreement with CERN.
[III] Also at An-Najah National University, Nablus; Palestine.
[IV] Also at Borough of Manhattan Community College, City University of New York, New York NY; United States of America.
[V] Also at Center for Interdisciplinary Research and Innovation (CIRI-AUTH), Thessaloniki; Greece.
[VI] Also at Centre of Physics of the Universities of Minho and Porto (CF-UM-UP); Portugal.
[VII] Also at CERN, Geneva; Switzerland.
[VIII] Also at Département de Physique Nucléaire et Corpusculaire, Université de Genève, Genève; Switzerland.
[IX] Also at Departament de Fisica de la Universitat Autonoma de Barcelona, Barcelona; Spain.
[X] Also at Department of Financial and Management Engineering, University of the Aegean, Chios; Greece.
[XI] Also at Department of Mathematical Sciences, University of South Africa, Johannesburg; South Africa.
[XII] Also at Department of Modern Physics and State Key Laboratory of Particle Detection and Electronics, University of Science and Technology of China, Hefei; China.
[XIII] Also at Department of Physics, Bolu Abant Izzet Baysal University, Bolu; Türkiye.
[XIV] Also at Department of Physics, King's College London, London; United Kingdom.
[XV] Also at Department of Physics, Stanford University, Stanford CA; United States of America.
[XVI] Also at Department of Physics, Stellenbosch University; South Africa.
[XVII] Also at Department of Physics, University of Fribourg, Fribourg; Switzerland.
[XVIII] Also at Department of Physics, University of Thessaly; Greece.

[XIX] Also at Department of Physics, Westmont College, Santa Barbara; United States of America.
[XX] Also at Faculty of Physics, Sofia University, 'St. Kliment Ohridski', Sofia; Bulgaria.
[XXI] Also at Faculty of Physics, University of Bucharest; Romania.
[XXII] Also at Hellenic Open University, Patras; Greece.
[XXIII] Also at Henan University; China.
[XXIV] Also at Imam Mohammad Ibn Saud Islamic University; Saudi Arabia.
[XXV] Also at Institucio Catalana de Recerca i Estudis Avancats, ICREA, Barcelona; Spain.
[XXVI] Also at Institut für Experimentalphysik, Universität Hamburg, Hamburg; Germany.
[XXVII] Also at Institute for Nuclear Research and Nuclear Energy (INRNE) of the Bulgarian Academy of Sciences, Sofia; Bulgaria.
[XXVIII] Also at Institute of Applied Physics, Mohammed VI Polytechnic University, Ben Guerir; Morocco.
[XXIX] Also at Institute of Particle Physics (IPP); Canada.
[XXX] Also at Institute of Physics and Technology, Mongolian Academy of Sciences, Ulaanbaatar; Mongolia.
[XXXI] Also at Institute of Physics, Azerbaijan Academy of Sciences, Baku; Azerbaijan.
[XXXII] Also at Institute of Theoretical Physics, Ilia State University, Tbilisi; Georgia.
[XXXIII] Also at Millennium Institute for Subatomic physics at high energy frontier (SAPHIR), Santiago; Chile.
[XXXIV] Also at National Institute of Physics, University of the Philippines Diliman (Philippines); Philippines.
[XXXV] Also at The Collaborative Innovation Center of Quantum Matter (CICQM), Beijing; China.
[XXXVI] Also at TRIUMF, Vancouver BC; Canada.
[XXXVII] Also at Università di Napoli Parthenope, Napoli; Italy.
[XXXVIII] Also at University of Chinese Academy of Sciences (UCAS), Beijing; China.
[XXXIX] Also at University of Colorado Boulder, Department of Physics, Colorado; United States of America.
[XL] Also at University of Siena; Italy.
[XLI] Also at Washington College, Chestertown, MD; United States of America.
[XLII] Also at Yeditepe University, Physics Department, Istanbul; Türkiye.

Collaboration Institutes

[1] Department of Physics, University of Adelaide, Adelaide, Australia
[2] Department of Physics, University of Alberta, Edmonton, AB, Canada
[3] Department of Physics, Ankara University, Ankara, Türkiye
[4] Division of Physics, TOBB University of Economics and Technology, Ankara, Türkiye
[5] LAPP, Université Savoie Mont Blanc, CNRS/IN2P3, Annecy, France
[6] APC, Université Paris Cité, CNRS/IN2P3, Paris, France
[7] High Energy Physics Division, Argonne National Laboratory, Argonne, IL, United States of America
[8] Department of Physics, University of Arizona, Tucson, AZ, United States of America
[9] Department of Physics, University of Texas at Arlington, Arlington, TX, United States of America
[10] Physics Department, National and Kapodistrian University of Athens, Athens, Greece
[11] Physics Department, National Technical University of Athens, Zografou, Greece
[12] Department of Physics, University of Texas at Austin, Austin, TX, United States of America
[13] Institute of Physics, Azerbaijan Academy of Sciences, Baku, Azerbaijan
[14] Institut de Física d'Altes Energies (IFAE), Barcelona Institute of Science and Technology, Barcelona, Spain
[15] Institute of High Energy Physics, Chinese Academy of Sciences, Beijing, China
[16] Physics Department, Tsinghua University, Beijing, China
[17] Institute of Physics, University of Belgrade, Belgrade, Serbia
[18] Department for Physics and Technology, University of Bergen, Bergen, Norway
[19] Physics Division, Lawrence Berkeley National Laboratory, Berkeley, CA, United States of America
[20] University of California, Berkeley, Berkeley, CA, United States of America
[21] Institut für Physik, Humboldt Universität zu Berlin, Berlin, Germany
[22] Albert Einstein Center for Fundamental Physics and Laboratory for High Energy Physics, University of Bern, Bern, Switzerland
[23] School of Physics and Astronomy, University of Birmingham, Birmingham, United Kingdom
[24] Department of Physics, Bogazici University, Istanbul, Türkiye
[25] Department of Physics Engineering, Gaziantep University, Gaziantep, Türkiye
[26] Department of Physics, Istanbul University, Istanbul, Türkiye
[27] Facultad de Ciencias y Centro de Investigaciónes, Universidad Antonio Nariño, Bogotá, Colombia
[28] Departamento de Física, Universidad Nacional de Colombia, Bogotá, Colombia
[29] Dipartimento di Fisica e Astronomia A. Righi, Università di Bologna, Bologna, Italy
[30] INFN Sezione di Bologna, Bologna, Italy
[31] Physikalisches Institut, Universität Bonn, Bonn, Germany
[32] Department of Physics, Boston University, Boston, MA, United States of America
[33] Department of Physics, Brandeis University, Waltham, MA, United States of America
[34] Transilvania University of Brasov, Brasov, Romania
[35] Horia Hulubei National Institute of Physics and Nuclear Engineering, Bucharest, Romania
[36] Department of Physics, Alexandru Ioan Cuza University of Iasi, Iasi, Romania
[37] National Institute for Research and Development of Isotopic and Molecular Technologies, Physics Department, Cluj-Napoca, Romania
[38] National University of Science and Technology Politechnica, Bucharest, Romania
[39] West University in Timisoara, Timisoara, Romania
[40] Faculty of Physics, University of Bucharest, Bucharest, Romania
[41] Faculty of Mathematics, Physics and Informatics, Comenius University, Bratislava, Slovak Republic
[42] Department of Subnuclear Physics, Institute of Experimental Physics of the Slovak Academy of Sciences, Kosice, Slovak Republic
[43] Physics Department, Brookhaven National Laboratory, Upton, NY, United States of America
[44] Universidad de Buenos Aires, Facultad de Ciencias Exactas y Naturales, Departamento de Física, y CONICET, Instituto de Física de Buenos Aires (IFIBA), Buenos Aires, Argentina
[45] California State University, CA, United States of America
[46] Cavendish Laboratory, University of Cambridge, Cambridge, United Kingdom
[47] Department of Physics, University of Cape Town, Cape Town, South Africa
[48] iThemba Labs, Western Cape, South Africa
[49] Department of Mechanical Engineering Science, University of Johannesburg, Johannesburg, South Africa
[50] National Institute of Physics, University of the Philippines Diliman, Philippines
[51] Department of Physics, Stellenbosch University, Matieland, South Africa
[52] University of South Africa, Department of Physics, Pretoria, South Africa
[53] University of Zululand, KwaDlangezwa, South Africa

[54] School of Physics, University of the Witwatersrand, Johannesburg, South Africa
[55] Department of Physics, Carleton University, Ottawa, ON, Canada
[56] Faculté des Sciences Ain Chock, Université Hassan II de Casablanca, Casablanca, Morocco
[57] Faculté des Sciences, Université Ibn-Tofail, Kénitra, Morocco
[58] Faculté des Sciences Semlalia, Université Cadi Ayyad, LPHEA-Marrakech, Marrakech, Morocco
[59] LPMR, Faculté des Sciences, Université Mohamed Premier, Oujda, Morocco
[60] Faculté des sciences, Université Mohammed V, Rabat, Morocco
[61] Institute of Applied Physics, Mohammed VI Polytechnic University, Ben Guerir, Morocco
[62] CERN, Geneva, Switzerland
[63] Affiliated with an institute formerly covered by a cooperation agreement with CERN
[64] Affiliated with an international laboratory covered by a cooperation agreement with CERN
[65] Enrico Fermi Institute, University of Chicago, Chicago, IL, United States of America
[66] LPC, Université Clermont Auvergne, CNRS/IN2P3, Clermont-Ferrand, France
[67] Nevis Laboratory, Columbia University, Irvington, NY, United States of America
[68] Niels Bohr Institute, University of Copenhagen, Copenhagen, Denmark
[69] Dipartimento di Fisica, Università della Calabria, Rende, Italy
[70] INFN Gruppo Collegato di Cosenza, Laboratori Nazionali di Frascati, Italy
[71] Physics Department, Southern Methodist University, Dallas, TX, United States of America
[72] National Centre for Scientific Research "Demokritos", Agia Paraskevi, Greece
[73] Department of Physics, Stockholm University, Stockholm, Sweden
[74] Oskar Klein Centre, Stockholm, Sweden
[75] Deutsches Elektronen-Synchrotron DESY, Hamburg and Zeuthen, Germany
[76] Fakultät Physik, Technische Universität Dortmund, Dortmund, Germany
[77] Institut für Kern- und Teilchenphysik, Technische Universität Dresden, Dresden, Germany
[78] Department of Physics, Duke University, Durham, NC, United States of America
[79] SUPA - School of Physics and Astronomy, University of Edinburgh, Edinburgh, United Kingdom
[80] INFN e Laboratori Nazionali di Frascati, Frascati, Italy
[81] Physikalisches Institut, Albert-Ludwigs-Universität Freiburg, Freiburg, Germany
[82] II. Physikalisches Institut, Georg-August-Universität Göttingen, Göttingen, Germany
[83] Département de Physique Nucléaire et Corpusculaire, Université de Genève, Genève, Switzerland
[84] Dipartimento di Fisica, Università di Genova, Genova, Italy
[85] INFN Sezione di Genova, Genova, Italy
[86] II. Physikalisches Institut, Justus-Liebig-Universität Giessen, Giessen, Germany
[87] SUPA - School of Physics and Astronomy, University of Glasgow, Glasgow, United Kingdom
[88] LPSC, Université Grenoble Alpes, CNRS/IN2P3, Grenoble INP, Grenoble, France
[89] Laboratory for Particle Physics and Cosmology, Harvard University, Cambridge, MA, United States of America
[90] Department of Modern Physics and State Key Laboratory of Particle Detection and Electronics, University of Science and Technology of China, Hefei, China
[91] Kirchhoff-Institut für Physik, Ruprecht-Karls-Universität Heidelberg, Heidelberg, Germany
[92] Physikalisches Institut, Ruprecht-Karls-Universität Heidelberg, Heidelberg, Germany
[93] Department of Physics, Chinese University of Hong Kong, Shatin, N.T., Hong Kong, China
[94] Department of Physics, University of Hong Kong, Hong Kong, China
[95] Department of Physics and Institute for Advanced Study, Hong Kong University of Science and Technology, Clear Water Bay, Kowloon, Hong Kong, China
[96] Department of Physics, National Tsing Hua University, Hsinchu, Taiwan
[97] IJCLab, Université Paris-Saclay, CNRS/IN2P3, Orsay, France
[98] Centro Nacional de Microelectrónica (IMB-CNM-CSIC), Barcelona, Spain
[99] Department of Physics, Indiana University, Bloomington, IN, United States of America
[100] INFN Gruppo Collegato di Udine, Sezione di Trieste, Udine, Italy
[101] ICTP, Trieste, Italy
[102] Dipartimento Politecnico di Ingegneria e Architettura, Università di Udine, Udine, Italy
[103] INFN Sezione di Lecce, Lecce, Italy
[104] Dipartimento di Matematica e Fisica, Università del Salento, Lecce, Italy
[105] INFN Sezione di Milano, Milano, Italy
[106] Dipartimento di Fisica, Università di Milano, Milano, Italy
[107] INFN Sezione di Napoli, Napoli, Italy
[108] Dipartimento di Fisica, Università di Napoli, Napoli, Italy
[109] INFN Sezione di Pavia, Pavia, Italy
[110] Dipartimento di Fisica, Università di Pavia, Pavia, Italy
[111] INFN Sezione di Pisa, Pisa, Italy
[112] Dipartimento di Fisica E. Fermi, Università di Pisa, Pisa, Italy
[113] INFN Sezione di Roma, Roma, Italy
[114] Dipartimento di Fisica, Sapienza Università di Roma, Roma, Italy
[115] INFN Sezione di Roma Tor Vergata, Roma, Italy
[116] Dipartimento di Fisica, Università di Roma Tor Vergata, Roma, Italy
[117] INFN Sezione di Roma Tre, Roma, Italy
[118] Dipartimento di Matematica e Fisica, Università Roma Tre, Roma, Italy
[119] INFN-TIFPA, Italy
[120] Università degli Studi di Trento, Trento, Italy
[121] Universität Innsbruck, Department of Astro and Particle Physics, Innsbruck, Austria
[122] University of Iowa, Iowa City, IA, United States of America
[123] Department of Physics and Astronomy, Iowa State University, Ames, IA, United States of America
[124] Istinye University, Sariyer, Istanbul, Türkiye
[125] Departamento de Engenharia Elétrica, Universidade Federal de Juiz de Fora (UFJF), Juiz de Fora, Brazil
[126] Universidade Federal do Rio De Janeiro COPPE/EE/IF, Rio de Janeiro, Brazil
[127] Instituto de Física, Universidade de São Paulo, São Paulo, Brazil
[128] Rio de Janeiro State University, Rio de Janeiro, Brazil
[129] Federal University of Bahia, Bahia, Brazil
[130] KEK, High Energy Accelerator Research Organization, Tsukuba, Japan
[131] Khalifa University of Science and Technology, Abu Dhabi, United Arab Emirates
[132] University of Sharjah, Sharjah, United Arab Emirates
[133] Graduate School of Science, Kobe University, Kobe, Japan
[134] AGH University of Krakow, Faculty of Physics and Applied Computer Science, Krakow, Poland
[135] Marian Smoluchowski Institute of Physics, Jagiellonian University, Krakow, Poland
[136] Institute of Nuclear Physics Polish Academy of Sciences, Krakow, Poland

[137] Faculty of Science, Kyoto University, Kyoto, Japan
[138] Research Center for Advanced Particle Physics and Department of Physics, Kyushu University, Fukuoka, Japan
[139] L2IT, Université de Toulouse, CNRS/IN2P3, UPS, Toulouse, France
[140] Instituto de Física La Plata, Universidad Nacional de La Plata and CONICET, La Plata, Argentina
[141] Physics Department, Lancaster University, Lancaster, United Kingdom
[142] Oliver Lodge Laboratory, University of Liverpool, Liverpool, United Kingdom
[143] Department of Experimental Particle Physics, Jožef Stefan Institute and Department of Physics, University of Ljubljana, Ljubljana, Slovenia
[144] Department of Physics and Astronomy, Queen Mary University of London, London, United Kingdom
[145] Department of Physics, Royal Holloway University of London, Egham, United Kingdom
[146] Department of Physics and Astronomy, University College London, London, United Kingdom
[147] Louisiana Tech University, Ruston, LA, United States of America
[148] Fysiska institutionen, Lunds universitet, Lund, Sweden
[149] Departamento de Física Teorica C-15 and CIAFF, Universidad Autónoma de Madrid, Madrid, Spain
[150] Institut für Physik, Universität Mainz, Mainz, Germany
[151] School of Physics and Astronomy, University of Manchester, Manchester, United Kingdom
[152] CPPM, Aix-Marseille Université, CNRS/IN2P3, Marseille, France
[153] Department of Physics, University of Massachusetts, Amherst, MA, United States of America
[154] Department of Physics, McGill University, Montreal, QC, Canada
[155] School of Physics, University of Melbourne, Victoria, Australia
[156] Department of Physics, University of Michigan, Ann Arbor, MI, United States of America
[157] Department of Physics and Astronomy, Michigan State University, East Lansing, MI, United States of America
[158] Group of Particle Physics, University of Montreal, Montreal, QC, Canada
[159] Fakultät für Physik, Ludwig-Maximilians-Universität München, München, Germany
[160] Max-Planck-Institut für Physik (Werner-Heisenberg-Institut), München, Germany
[161] Graduate School of Science and Kobayashi-Maskawa Institute, Nagoya University, Nagoya, Japan
[162] Department of Physics, Nanjing University, Nanjing, China
[163] School of Science, Shenzhen Campus of Sun Yat-sen University, Shenzhen, China
[164] University of Chinese Academy of Science (UCAS), Beijing, China
[165] Department of Physics and Astronomy, University of New Mexico, Albuquerque, NM, United States of America
[166] Institute for Mathematics, Astrophysics and Particle Physics, Radboud University/Nikhef, Nijmegen, Netherlands
[167] Nikhef National Institute for Subatomic Physics and University of Amsterdam, Amsterdam, Netherlands
[168] Department of Physics, Northern Illinois University, DeKalb, IL, United States of America
[169] New York University Abu Dhabi, Abu Dhabi, United Arab Emirates
[170] United Arab Emirates University, Al Ain, United Arab Emirates
[171] Department of Physics, New York University, New York, NY, United States of America
[172] Ochanomizu University, Otsuka, Bunkyo-ku, Tokyo, Japan
[173] Ohio State University, Columbus, OH, United States of America
[174] Homer L. Dodge Department of Physics and Astronomy, University of Oklahoma, Norman, OK, United States of America
[175] Department of Physics, Oklahoma State University, Stillwater, OK, United States of America
[176] Palacký University, Joint Laboratory of Optics, Olomouc, Czech Republic
[177] Institute for Fundamental Science, University of Oregon, Eugene, OR, United States of America
[178] Graduate School of Science, University of Osaka, Osaka, Japan
[179] Department of Physics, University of Oslo, Oslo, Norway
[180] Department of Physics, Oxford University, Oxford, United Kingdom
[181] LPNHE, Sorbonne Université, Université Paris Cité, CNRS/IN2P3, Paris, France
[182] Department of Physics, University of Pennsylvania, Philadelphia, PA, United States of America
[183] Department of Physics and Astronomy, University of Pittsburgh, Pittsburgh, PA, United States of America
[184] Laboratório de Instrumentação e Física Experimental de Partículas - LIP, Lisboa, Portugal
[185] Departamento de Física, Faculdade de Ciências, Universidade de Lisboa, Lisboa, Portugal
[186] Departamento de Física, Universidade de Coimbra, Coimbra, Portugal
[187] Centro de Física Nuclear da Universidade de Lisboa, Lisboa, Portugal
[188] Departamento de Física, Escola de Ciências, Universidade do Minho, Braga, Portugal
[189] Departamento de Física Teórica y del Cosmos, Universidad de Granada, Granada, Spain
[190] Departamento de Física, Instituto Superior Técnico, Universidade de Lisboa, Lisboa, Portugal
[191] Institute of Physics of the Czech Academy of Sciences, Prague, Czech Republic
[192] Czech Technical University in Prague, Prague, Czech Republic
[193] Charles University, Faculty of Mathematics and Physics, Prague, Czech Republic
[194] Particle Physics Department, Rutherford Appleton Laboratory, Didcot, United Kingdom
[195] IRFU, CEA, Université Paris-Saclay, Gif-sur-Yvette, France
[196] Santa Cruz Institute for Particle Physics, University of California Santa Cruz, Santa Cruz, CA, United States of America
[197] Departamento de Física, Pontificia Universidad Católica de Chile, Santiago, Chile
[198] Millennium Institute for Subatomic physics at high energy frontier (SAPHIR), Santiago, Chile
[199] Instituto de Investigación Multidisciplinario en Ciencia y Tecnología, y Departamento de Física, Universidad de La Serena, La Serena, Chile
[200] Universidad Andres Bello, Department of Physics, Santiago, Chile
[201] Universidad San Sebastian, Recoleta, Chile
[202] Instituto de Alta Investigación, Universidad de Tarapacá, Arica, Chile
[203] Departamento de Física, Universidad Técnica Federico Santa María, Valparaíso, Chile
[204] Department of Physics, Institute of Science, Tokyo, Japan
[205] Department of Physics, University of Washington, Seattle, WA, United States of America
[206] Institute of Frontier and Interdisciplinary Science and Key Laboratory of Particle Physics and Particle Irradiation (MOE), Shandong University, Qingdao, China
[207] School of Physics, Zhengzhou University, Zhengzhou, China
[208] State Key Laboratory of Dark Matter Physics, School of Physics and Astronomy, Shanghai Jiao Tong University, Key Laboratory for Particle Astrophysics and Cosmology (MOE), SKLPPC, Shanghai, China
[209] State Key Laboratory of Dark Matter Physics, Tsung-Dao Lee Institute, Shanghai Jiao Tong University, Shanghai, China
[210] Department of Physics and Astronomy, University of Sheffield, Sheffield, United Kingdom
[211] Department of Physics, Shinshu University, Nagano, Japan
[212] Department Physik, Universität Siegen, Siegen, Germany
[213] Department of Physics, Simon Fraser University, Burnaby, BC, Canada
[214] SLAC National Accelerator Laboratory, Stanford, CA, United States of America

[215] Department of Physics, Royal Institute of Technology, Stockholm, Sweden
[216] Departments of Physics and Astronomy, Stony Brook University, Stony Brook, NY, United States of America
[217] Department of Physics and Astronomy, University of Sussex, Brighton, United Kingdom
[218] School of Physics, University of Sydney, Sydney, Australia
[219] Institute of Physics, Academia Sinica, Taipei, Taiwan
[220] E. Andronikashvili Institute of Physics, Iv. Javakhishvili Tbilisi State University, Tbilisi, Georgia
[221] High Energy Physics Institute, Tbilisi State University, Tbilisi, Georgia
[222] University of Georgia, Tbilisi, Georgia
[223] Department of Physics, Technion, Israel Institute of Technology, Haifa, Israel
[224] Raymond and Beverly Sackler School of Physics and Astronomy, Tel Aviv University, Tel Aviv, Israel
[225] Department of Physics, Aristotle University of Thessaloniki, Thessaloniki, Greece
[226] International Center for Elementary Particle Physics and Department of Physics, University of Tokyo, Tokyo, Japan
[227] Graduate School of Science and Technology, Tokyo Metropolitan University, Tokyo, Japan
[228] Department of Physics, University of Toronto, Toronto, ON, Canada
[229] TRIUMF, Vancouver, BC, Canada
[230] Department of Physics and Astronomy, York University, Toronto, ON, Canada
[231] Division of Physics and Tomonaga Center for the History of the Universe, Faculty of Pure and Applied Sciences, University of Tsukuba, Tsukuba, Japan
[232] Department of Physics and Astronomy, Tufts University, Medford, MA, United States of America
[233] Department of Physics and Astronomy, University of California Irvine, Irvine, CA, United States of America
[234] University of West Attica, Athens, Greece
[235] Department of Physics and Astronomy, University of Uppsala, Uppsala, Sweden
[236] Department of Physics, University of Illinois, Urbana, IL, United States of America
[237] Instituto de Física Corpuscular (IFIC), Centro Mixto Universidad de Valencia - CSIC, Valencia, Spain
[238] Department of Physics, University of British Columbia, Vancouver, BC, Canada
[239] Department of Physics and Astronomy, University of Victoria, Victoria, BC, Canada
[240] Fakultät für Physik und Astronomie, Julius-Maximilians-Universität Würzburg, Würzburg, Germany
[241] Department of Physics, University of Warwick, Coventry, United Kingdom
[242] Waseda University, Tokyo, Japan
[243] Department of Particle Physics and Astrophysics, Weizmann Institute of Science, Rehovot, Israel
[244] Department of Physics, University of Wisconsin, Madison, WI, United States of America
[245] Fakultät für Mathematik und Naturwissenschaften, Fachgruppe Physik, Bergische Universität Wuppertal, Wuppertal, Germany
[246] Department of Physics, Yale University, New Haven, CT, United States of America
[247] Yerevan Physics Institute, Yerevan, Armenia

References

[1] F. Englert, R. Brout, Broken symmetry and the mass of gauge vector mesons, Phys. Rev. Lett. 13 (1964) 321, https://doi.org/10.1103/PhysRevLett.13.321

[2] P.W. Higgs, Broken symmetries, massless particles and gauge fields, Phys. Lett. 12 (1964) 132, https://doi.org/10.1016/0031-9163(64)91136-9

[3] P.W. Higgs, Broken symmetries and the masses of gauge Bosons, Phys. Rev. Lett. 13 (1964) 508, https://doi.org/10.1103/PhysRevLett.13.508

[4] G.S. Guralnik, C.R. Hagen, T.W.B. Kibble, Global conservation laws and massless particles, Phys. Rev. Lett. 13 (1964) 585, https://doi.org/10.1103/PhysRevLett.13.585

[5] P.W. Higgs, Spontaneous symmetry breakdown without massless Bosons, Phys. Rev. 145 (1966) 1156, https://doi.org/10.1103/PhysRev.145.1156

[6] T.W.B. Kibble, Symmetry breaking in non-Abelian gauge theories, Phys. Rev. 155 (1967) 1554, https://doi.org/10.1103/PhysRev.155.1554

[7] ATLAS Collaboration, Observation of a new particle in the search for the standard model Higgs boson with the ATLAS detector at the LHC, Phys. Lett. B 716 (2012) 1. arXiv:1207.7214, https://doi.org/10.1016/j.physletb.2012.08.020

[8] CMS Collaboration, Observation of a new boson at a mass of 125 GeV with the CMS experiment at the LHC, Phys. Lett. B 716 (2012) 30. arXiv:1207.7235, https://doi.org/10.1016/j.physletb.2012.08.021

[9] L. Evans, P. Bryant, LHC machine, JINST 3 (2008) S08001, https://doi.org/10.1088/1748-0221/3/08/S08001

[10] B. Horn, The Higgs field and early universe cosmology: a (Brief) review, MDPI Phys. 2 (3) (2020) 503–520. arXiv:2007.10377, https://doi.org/10.3390/physics2030028

[11] M. Reichert, A. Eichhorn, H. Gies, J.M. Pawlowski, T. Plehn, M.M. Scherer, Probing baryogenesis through the Higgs Boson self-coupling, Phys. Rev. D 97 (7) (2018) 075008. arXiv:1711.00019, https://doi.org/10.1103/PhysRevD.97.075008

[12] A. Noble, M. Perelstein, Higgs self-coupling as a probe of the electroweak phase transition, Phys. Rev. D 78 (2008) 063518. arXiv:0711.3018, https://doi.org/10.1103/PhysRevD.78.063518

[13] T. Markkanen, A. Rajantie, S. Stopyra, Cosmological aspects of Higgs vacuum metastability, Front. Astron. Space Sci. 5 (2018) 40. arXiv:1809.06923, https://doi.org/10.3389/fspas.2018.00040

[14] ATLAS Collaboration, Search for triple Higgs boson production in the $6b$ final state using pp collisions at $\sqrt{s} = 13$ TeV with the ATLAS detector, Phys. Rev. D 111 (2025) 032006. arXiv:2411.02040, https://doi.org/10.1103/PhysRevD.111.032006

[15] M. Grazzini, G. Heinrich, S. Jones, S. Kallweit, M. Kerner, J.M. Lindert, J. Mazzitelli, Higgs boson pair production at NNLO with top quark mass effects, JHEP 05 (2018) 059. arXiv:1803.02463, https://doi.org/10.1007/JHEP05(2018)059

[16] S. Dawson, S. Dittmaier, M. Spira, Neutral Higgs-boson pair production at hadron colliders: QCD corrections, Phys. Rev. D 58 (1998). 115012. arXiv:hep-ph/9805244, https://doi.org/10.1103/PhysRevD.58.115012

[17] S. Borowka, N. Greiner, G. Heinrich, S. Jones, M. Kerner, J. Schlenk, U. Schubert, T. Zirke, Higgs Boson pair production in gluon fusion at next-to-leading order with full top-quark mass dependence, Phys. Rev. Lett. 117 (1) (2016) 012001. arXiv:1604.06447, https://doi.org/10.1103/PhysRevLett.117.012001

[18] J. Baglio, F. Campanario, S. Glaus, M. Mühlleitner, M. Spira, J. Streicher, Gluon fusion into Higgs pairs at NLO QCD and the top mass scheme, Eur. Phys. J. C 79 (6) (2019) 459. arXiv:1811.05692, https://doi.org/10.1140/epjc/s10052-019-6973-3

[19] D. de Florian, J. Mazzitelli, Higgs Boson pair production at next-to-next-to-leading order in QCD, Phys. Rev. Lett. 111 (2013) 201801. arXiv:1309.6594, https://doi.org/10.1103/PhysRevLett.111.201801

[20] D.Y. Shao, C.S. Li, H.T. Li, J. Wang, Threshold resummation effects in Higgs boson pair production at the LHC, JHEP 07 (2013) 169. arXiv:1301.1245, https://doi.org/10.1007/JHEP07(2013)169

[21] D. de Florian, J. Mazzitelli, Higgs pair production at next-to-next-to-leading logarithmic accuracy at the LHC, JHEP 09 (2015) 053. arXiv:1505.07122, https://doi.org/10.1007/JHEP09(2015)053

[22] J. Baglio, F. Campanario, S. Glaus, M. Mühlleitner, J. Ronca, M. Spira, $gg \to HH$: Combined uncertainties, Phys. Rev. D 103 (5) (2021) 056002. arXiv:2008.11626 https://doi.org/10.1103/PhysRevD.103.056002

[23] G. Heinrich, J. Lang, L. Scyboz, SMEFT predictions for gg → hh at full NLO QCD and truncation uncertainties, JHEP 08 (2022) 079. arXiv:2204.13045, https://doi.org/10.1007/JHEP08(2022)079

[24] E. Bagnaschi, G. Degrassi, R. Gröber, Higgs boson pair production at NLO in the POWHEG approach and the top quark mass uncertainties, Eur. Phys. J. C 83 (11) (2023) 1054. arXiv:2309.10525, https://doi.org/10.1140/epjc/s10052-023-12238-8

[25] J. Baglio, A. Djouadi, R. Gröber, M.M. Mühlleitner, J. Quevillon, M. Spira, The measurement of the Higgs self-coupling at the LHC: theoretical status, JHEP 04 (4) (2013) 151. arXiv:1212.5581, https://doi.org/10.1007/jhep04(2013)151

[26] L.-S. Ling, R.-Y. Zhang, W.-G. Ma, L. Guo, W.-H. Li, X.-Z. Li, NNLO QCD corrections to Higgs pair production via vector boson fusion at hadron colliders, Phys. Rev. D 89 (2014) 073001. arXiv:1401.7754, https://doi.org/10.1103/PhysRevD.89.073001

[27] F.A. Dreyer, A. Karlberg, Vector-Boson fusion Higgs pair production at N^{3}LO, Phys. Rev. D 98 (11) (2018) 114016. arXiv:1811.07906, https://doi.org/10.1103/PhysRevD.98.114016

[28] F.A. Dreyer, A. Karlberg, J.-N. Lang, M. Pellen, Precise predictions for double-Higgs production via vector-boson fusion, Eur. Phys. J. C 80 (11) (2020) 1037. arXiv:2005.13341, https://doi.org/10.1140/epjc/s10052-020-08610-7

[29] ATLAS Collaboration, Studies of new Higgs boson interactions through nonresonant HH production in the $b\bar{b}\gamma\gamma$ final state in pp collisions at $\sqrt{s} = 13$ TeV with the ATLAS detector, JHEP 01 (2024) 066. arXiv:2310.12301, https://doi.org/10.1007/JHEP01(2024)066

[30] ATLAS Collaboration, Transforming jet flavour tagging at ATLAS (2025). 2505.19689

[31] ATLAS Collaboration, Calibration of the light-flavour jet mistagging efficiency of the b-tagging algorithms with Z+jets events using $139\,\mathrm{fb}^{-1}$ of ATLAS proton–proton collision data at $\sqrt{s} = 13$ TeV, Eur. Phys. J. C 83 (2023) 728. arXiv:2301.06319, https://doi.org/10.1140/epjc/s10052-023-11736-z

[32] ATLAS Collaboration, Measurement of the c-jet mistagging efficiency in $t\bar{t}$ events using pp collision data at $\sqrt{s} = 13$ TeV collected with the ATLAS detector, Eur. Phys. J. C 82 (2022) 95. arXiv:2109.10627, https://doi.org/10.1140/epjc/s10052-021-09843-w

[33] ATLAS Collaboration, ATLAS B-jet identification performance and efficiency measurement with $t\bar{t}$ events in pp collisions at $\sqrt{s} = 13$ TeV, Eur. Phys. J. C 79 (2019) 970. arXiv:1907.05120, https://doi.org/10.1140/epjc/s10052-019-7450-8

[34] CMS Collaboration, Search for nonresonant Higgs boson pair production in final states with two bottom quarks and two photons in proton–proton collisions at $\sqrt{s} = 13$ TeV, JHEP 03 (2021) 257. arXiv:2011.12373, https://doi.org/10.1007/JHEP03(2021)257

[35] ATLAS Collaboration, Search for nonresonant pair production of Higgs bosons in the $b\bar{b}b\bar{b}$ final state in pp collisions at $\sqrt{s} = 13$ TeV with the ATLAS detector, Phys. Rev. D 108 (2023) 052003. arXiv:2301.03212, https://doi.org/10.1103/PhysRevD.108.052003

[36] ATLAS Collaboration, Search for pair production of boosted Higgs bosons via vector-boson fusion in the $b\bar{b}b\bar{b}$ final state using pp collisions at $\sqrt{s} = 13$ TeV with the ATLAS detector, Phys. Lett. B 858 (2024) 139007. arXiv:2404.17193, https://doi.org/10.1016/j.physletb.2024.139007

[37] ATLAS Collaboration, Search for the non-resonant production of Higgs boson pairs via gluon fusion and vector-boson fusion in the $b\bar{b}\tau^+\tau^-$ final state in proton–proton collisions at $\sqrt{s} = 13$ TeV with the ATLAS detector, Phys. Rev. D 110 (2024) 032012. arXiv:2404.12660, https://doi.org/10.1103/PhysRevD.110.032012

[38] ATLAS Collaboration, Search for non-resonant Higgs boson pair production in final states with leptons, taus, and photons in pp collisions at $\sqrt{s} = 13$ TeV with the ATLAS detector, JHEP 08 (2024) 164. arXiv:2405.20040, https://doi.org/10.1007/JHEP08(2024)164

[39] ATLAS Collaboration, Search for non-resonant Higgs boson pair production in the $2b + 2\ell + E_{\mathrm{T}}^{\mathrm{miss}}$ final state in pp collisions at $\sqrt{s} = 13$TeV with the ATLAS detector, JHEP 02 (2024) 037. arXiv:2310.11286, https://doi.org/10.1007/JHEP02(2024)037

[40] CMS Collaboration, Search for nonresonant Higgs boson pair production in final state with two bottom quarks and two tau leptons in proton–proton collisions at $\sqrt{s} = 13$ TeV, Phys. Lett. B 842 (2023) 137531. arXiv:2206.09401, https://doi.org/10.1016/j.physletb.2022.137531

[41] CMS Collaboration, Search for Higgs Boson pair production in the four b quark final state in proton–Proton collisions at $\sqrt{s} = 13$ TeV, Phys. Rev. Lett. 129 (2022) 081802. arXiv:2202.09617, https://doi.org/10.1103/PhysRevLett.129.081802

[42] CMS Collaboration, Search for Higgs boson pair production with one associated vector boson in proton–proton collisions at $\sqrt{s} = 13$ TeV, JHEP 10 (2024) 061. arXiv:2404.08462https://doi.org/10.1007/JHEP10(2024)061

[43] CMS Collaboration, Search for Higgs boson pairs decaying to WW^*WW^*, $WW^*\tau\tau$, and $\tau\tau\tau\tau$ in proton–proton collisions at $\sqrt{s} = 13$ TeV, JHEP 07 (2023) 095. arXiv:2206.10268, https://doi.org/10.1007/JHEP07(2023)095

[44] CMS Collaboration, Search for Higgs boson pair production in the $b\bar{b}W^+W^-$ decay mode in proton–proton collisions at $\sqrt{s} = 13$ TeV, JHEP 07 (2024) 293. arXiv:2403.09430, https://doi.org/10.1007/JHEP07(2024)293

[45] ATLAS Collaboration, Combination of searches for Higgs Boson pair production in pp collisions at $\sqrt{s} = 13$ TeV with the ATLAS detector, Phys. Rev. Lett. 133 (2024) 101801. arXiv:2406.09971, https://doi.org/10.1103/PhysRevLett.133.101801

[46] CMS Collaboration, A portrait of the Higgs boson by the CMS experiment ten years after the discovery, Nature 607 (2022) 60–68. arXiv:2207.00043, https://doi.org/10.1038/s41586-022-04892-x

[47] CMS Collaboration, Constraints on the Higgs boson self-coupling from the combination of single and double Higgs boson production in proton–proton collisions at $\sqrt{s} = 13$ TeV, Phys. Lett. B 861 (2025) 139210. arXiv:2407.13554, https://doi.org/10.1016/j.physletb.2024.139210

[48] ATLAS Collaboration, The ATLAS experiment at the CERN large hadron collider, JINST 3 (2008) S08003, https://doi.org/10.1088/1748-0221/3/08/S08003

[49] ATLAS Collaboration, The ATLAS experiment at the CERN large hadron collider: a description of the detector configuration for Run 3, JINST 19 (2024) P05063. arXiv:2305.16623https://doi.org/10.1088/1748-0221/19/05/P05063

[50] ATLAS Collaboration, Performance of the ATLAS trigger system in 2015, Eur. Phys. J. C 77 (2017) 317. arXiv:1611.09661, https://doi.org/10.1140/epjc/s10052-017-4852-3

[51] ATLAS Collaboration, The ATLAS trigger system for LHC Run 3 and trigger performance in 2022, JINST 19 (2024) P06029. arXiv:2401.06630, https://doi.org/10.1088/1748-0221/19/06/P06029

[52] ATLAS Collaboration, Software and computing for Run 3 of the ATLAS experiment at the LHC, Eur. Phys. J. C 85 (2025) 234. arXiv:2404.06335, https://doi.org/10.1140/epjc/s10052-024-13701-w

[53] ATLAS Collaboration, ATLAS data quality operations and performance for 2015–2018 data-taking, JINST 15 (2020) P04003. arXiv:1911.04632, https://doi.org/10.1088/1748-0221/15/04/P04003

[54] ATLAS Collaboration, Luminosity determination in pp collisions at $\sqrt{s} = 13$ TeV using the ATLAS detector at the LHC, Eur. Phys. J. C 83 (2023) 982. arXiv:2212.09379, https://doi.org/10.1140/epjc/s10052-023-11747-w

[55] P. Nason, A new method for combining NLO QCD with shower Monte Carlo algorithms, JHEP 11 (2004) 040. arXiv:hep-ph/0409146, https://doi.org/10.1088/1126-6708/2004/11/040

[56] S. Frixione, P. Nason, C. Oleari, Matching NLO QCD computations with parton shower simulations: the POWHEG method, JHEP 11 (2007) 070. arXiv:0709.2092, https://doi.org/10.1088/1126-6708/2007/11/070

[57] S. Alioli, P. Nason, C. Oleari, E. Re, A general framework for implementing NLO calculations in shower Monte Carlo programs: the POWHEG BOX, JHEP 06 (2010) 043. arXiv:1002.2581, https://doi.org/10.1007/JHEP06(2010)043

[58] G. Heinrich, S.P. Jones, M. Kerner, G. Luisoni, E. Vryonidou, NLO predictions for Higgs boson pair production with full top quark mass dependence matched to parton showers, JHEP 08 (2017) 088. arXiv:1703.09252, https://doi.org/10.1007/JHEP08(2017)088

[59] G. Heinrich, S.P. Jones, M. Kerner, G. Luisoni, L. Scyboz, Probing the trilinear Higgs boson coupling in di-Higgs production at NLO QCD including parton shower effects, JHEP 06 (2019) 066. arXiv:1903.08137, https://doi.org/10.1007/JHEP06(2019)066

[60] J. Butterworth, et al., PDF4LHC recommendations for LHC Run II, J. Phys. G 43 (2016) 023001. arXiv:1510.03865, https://doi.org/10.1088/0954-3899/43/2/023001

[61] J. Alwall, R. Frederix, S. Frixione, V. Hirschi, F. Maltoni, O. Mattelaer, H.-S. Shao, T. Stelzer, P. Torrielli, M. Zaro, The automated computation of tree-level and next-to-leading order differential cross sections, and their matching to parton shower simulations, JHEP 07 (2014) 079. arXiv:1405.0301, https://doi.org/10.1007/JHEP07(2014)079

[62] NNPDF Collaboration, R.D. Ball, et al., Parton distributions for the LHC run II, JHEP 04 (2015) 040. arXiv:1410.8849, https://doi.org/10.1007/JHEP04(2015)040

[63] C. Bierlich, S. Chakraborty, N. Desai, L. Gellersen, I. Helenius, P. Ilten, L. Lönnblad, S. Mrenna, S. Prestel, C.T. Preuss, T. Sjöstrand, P. Skands, M. Utheim, R. Verheyen, A comprehensive guide to the physics and usage of PYTHIA 8.3, SciPost Phys. Codebases (2022) 8. arXiv:2203.11601, https://doi.org/10.21468/SciPostPhysCodeb.8

[64] ATLAS Collaboration, ATLAS Pythia 8 tunes to 7 TeV data, ATL-PHYS-PUB-2014-021, 2014. https://cds.cern.ch/record/1966419.

[65] K. Hamilton, P. Nason, E. Re, G. Zanderighi, NNLOPS simulation of Higgs boson production, JHEP 10 (2013) 222. arXiv:1309.0017, https://doi.org/10.1007/JHEP10(2013)222

[66] K. Hamilton, P. Nason, G. Zanderighi, Finite quark-mass effects in the NNLOPS POWHEG + MiNLO Higgs generator, JHEP 05 (2015) 140. arXiv:1501.04637, https://doi.org/10.1007/JHEP05(2015)140

[67] ATLAS Collaboration, Measurement of the Z/γ^* boson transverse momentum distribution in pp collisions at $\sqrt{s} = 7$ TeV with the ATLAS detector, JHEP 09 (2014) 145. arXiv:1406.3660, https://doi.org/10.1007/JHEP09(2014)145

[68] P. Nason, C. Oleari, NLO Higgs boson production via vector-boson fusion matched with shower in POWHEG, JHEP 02 (2010) 037. arXiv:0911.5299, https://doi.org/10.1007/JHEP02(2010)037

[69] G. Luisoni, P. Nason, C. Oleari, F. Tramontano, $HW^{\pm}/HZ\, +\, 0$ and 1 jet at NLO with the POWHEG BOX interfaced to GoSam and their merging within MiNLO, JHEP 10 (2013) 083. arXiv:1306.2542, https://doi.org/10.1007/JHEP10(2013)083

[70] H.B. Hartanto, B. Jäger, L. Reina, D. Wackeroth, Higgs boson production in association with top quarks in the POWHEG BOX, Phys. Rev. D 91 (9) (2015) 094003. arXiv:1501.04498, https://doi.org/10.1103/PhysRevD.91.094003

[71] B. Jäger, L. Reina, D. Wackeroth, Higgs boson production in association with b jets in the POWHEG BOX, Phys. Rev. D 93 (1) (2016) 014030. arXiv:1509.05843, https://doi.org/10.1103/PhysRevD.93.014030

[72] D.J. Lange, The EvtGen particle decay simulation package, Nucl. Instrum. Meth. A 462 (2001) 152, https://doi.org/10.1016/S0168-9002(01)00089-4

[73] E. Bothmann, et al., Event generation with Sherpa 2.2, SciPost Phys. 7 (3) (2019) 034. arXiv:1905.09127https://doi.org/10.21468/SciPostPhys.7.3.034

[74] ATLAS Collaboration, The ATLAS simulation infrastructure, Eur. Phys. J. C 70 (2010) 823. arXiv:1005.4568, https://doi.org/10.1140/epjc/s10052-010-1429-9

[75] S. Agostinelli, et al., Geant4 – a simulation toolkit, Nucl. Instrum. Meth. A 506 (2003) 250, https://doi.org/10.1016/S0168-9002(03)01368-8

[76] ATLAS Collaboration, AtlFast3: the next generation of fast simulation in ATLAS, Comput. Softw. Big Sci. 6 (2022) 7. arXiv:2109.02551, https://doi.org/10.1007/s41781-021-00079-7

[77] ATLAS Collaboration, Combined measurement of the Higgs Boson mass from the $H \to \gamma\gamma$ and $H \to ZZ^* \to 4\ell$ decay channels with the ATLAS detector using $\sqrt{s} = 7, 8,$ and13 TeV pp collision data, Phys. Rev. Lett. 131 (2023) 251802. arXiv:2308.04775, https://doi.org/10.1103/PhysRevLett.131.251802

[78] ATLAS Collaboration, Measurement of the $H \to \gamma\gamma$ and $H \to ZZ^* \to 4\ell$ cross-sections in pp collisions at $\sqrt{s} = 13.6$ TeV with the ATLAS detector, Eur. Phys. J. C 84 (2024) 78. arXiv:2306.11379, https://doi.org/10.1140/epjc/s10052-023-12130-5

[79] ATLAS Collaboration, 2025, https://zenodo.org/records/15927813.

[80] ATLAS Collaboration, Performance of electron and photon triggers in ATLAS during LHC Run 2, Eur. Phys. J. C 80 (2020) 47. arXiv:1909.00761, https://doi.org/10.1140/epjc/s10052-019-7500-2

[81] ATLAS Collaboration, Vertex Reconstruction Performance of the ATLAS Detector at $\sqrt{s} = 13$ TeV, ATL-PHYS-PUB-2015-026, 2015. https://cds.cern.ch/record/2037717.

[82] ATLAS Collaboration, Electron and photon performance measurements with the ATLAS detector using the 2015–2017 LHC proton–proton collision data, JINST 14 (2019) P12006. arXiv:1908.00005, https://doi.org/10.1088/1748-0221/14/12/P12006

[83] ATLAS Collaboration, Electron and photon energy calibration with the ATLAS detector using LHC Run 2 data, JINST 19 (2024) P02009. arXiv:2309.05471, https://doi.org/10.1088/1748-0221/19/02/P02009

[84] ATLAS Collaboration, Electron and photon efficiencies in LHC Run 2 with the ATLAS experiment, JHEP 05 (2024) 162. arXiv:2308.13362, https://doi.org/10.1007/JHEP05(2024)162

[85] M. Cacciari, G.P. Salam, G. Soyez, FastJet user manual, Eur. Phys. J. C 72 (2012) 1896. arXiv:1111.6097https://doi.org/10.1140/epjc/s10052-012-1896-2

[86] M. Cacciari, G.P. Salam, G. Soyez, The anti-k_t jet clustering algorithm, JHEP 04 (2008) 063. arXiv:0802.1189, https://doi.org/10.1088/1126-6708/2008/04/063

[87] ATLAS Collaboration, Performance of pile-up mitigation techniques for jets in pp collisions at $\sqrt{s} = 8$ TeV using the ATLAS detector, Eur. Phys. J. C 76 (2016) 581. arXiv:1510.03823, https://doi.org/10.1140/epjc/s10052-016-4395-z

[88] ATLAS Collaboration, Forward jet vertex tagging using the particle flow algorithm, ATL-PHYS-PUB-2019-026, 2019. https://cds.cern.ch/record/2683100.

[89] ATLAS Collaboration, Measurements of WH and ZH production with Higgs boson decays into bottom quarks and direct constraints on the charm Yukawa coupling in 13 TeV pp collisions with the ATLAS detector, JHEP 04 (2025) 075. arXiv:2410.19611, https://doi.org/10.1007/JHEP04(2025)075

[90] ATLAS Collaboration, Muon reconstruction and identification efficiency in ATLAS using the full Run 2 pp collision data set at $\sqrt{s} = 13$ TeV, Eur. Phys. J. C 81 (2021) 578. arXiv:2012.00578, https://doi.org/10.1140/epjc/s10052-021-09233-2

[91] ATLAS Collaboration, Measurement of the properties of Higgs boson production at $\sqrt{s} = 13$ TeV in the $H \to \gamma\gamma$ channel using 139 fb^{-1} of pp collision data with the ATLAS experiment, JHEP 07 (2023) 088. arXiv:2207.00348, https://doi.org/10.1007/JHEP07(2023)088

[92] J. Alison, et al., Higgs boson potential at colliders: status and perspectives, Rev. Phys. 5 (2020) 100045. arXiv:1910.00012, https://doi.org/10.1016/j.revip.2020.100045

[93] ATLAS Collaboration, Search for Higgs boson pair production in the two bottom quarks plus two photons final state in pp collisions at $\sqrt{s} = 13$ TeV with the ATLAS detector, Phys. Rev. D 106 (2022) 052001. arXiv:2112.11876, https://doi.org/10.1103/PhysRevD.106.052001

[94] T. Chen, C. Guestrin, XGBoost: A Scalable Tree Boosting System, 2016. 1603.02754, https://doi.org/10.1145/2939672.2939785

[95] G. Cowan, K. Cranmer, E. Gross, O. Vitells, Asymptotic formulae for likelihood-based tests of new physics, Eur. Phys. J. C 71 (2011) 1554. arXiv:1007.1727, https://doi.org/10.1140/epjc/s10052-011-1554-0

[96] M. Oreglia, A Study of the Reactions $\psi' \to \gamma\gamma\psi$, Appendix D. Ph.D. thesis, Stanford University, SLAC-R-0236 (1980), https://www-public.slac.stanford.edu/sciDoc/docMeta.aspx?slacPubNumber=slac-r-236.

[97] ATLAS Collaboration, Measurement of Higgs boson production in the diphoton decay channel in pp collisions at center-of-mass energies of 7 and 8 TeV with the ATLAS detector, Phys. Rev. D 90 (2014) 112015. arXiv:1408.7084, https://doi.org/10.1103/PhysRevD.90.112015

[98] ATLAS Collaboration, Search for scalar diphoton resonances in the mass range 65–600 GeV with the ATLAS detector in pp collision data at $\sqrt{s} = 8$ TeV, Phys. Rev. Lett. 113 (2014) 171801. arXiv:1407.6583, https://doi.org/10.1103/PhysRevLett.113.171801

[99] ATLAS Collaboration, Jet energy scale and resolution measured in proton–proton collisions at $\sqrt{s} = 13$ TeV with the ATLAS detector, Eur. Phys. J. C 81 (2021) 689. arXiv:2007.02645, https://doi.org/10.1140/epjc/s10052-021-09402-3

[100] ATLAS Collaboration, ATLAS flavour-tagging algorithms for the LHC Run 2 pp collision dataset, Eur. Phys. J. C 83 (2023) 681. arXiv:2211.16345, https://doi.org/10.1140/epjc/s10052-023-11699-1

[101] ATLAS Collaboration, Measurements of inclusive and differential fiducial cross-sections of $t\bar{t}$ production with additional heavy-flavour jets in proton–proton collisions at $\sqrt{s} = 13$ TeV with the ATLAS detector, JHEP 04 (2019) 046. arXiv:1811.12113, https://doi.org/10.1007/JHEP04(2019)046

[102] ATLAS Collaboration, Study of heavy-flavor quarks produced in association with top-quark pairs at $\sqrt{s} = 7$ TeV using the ATLAS detector, Phys. Rev. D 89 (2014) 072012. arXiv:1304.6386, https://doi.org/10.1103/PhysRevD.89.072012

[103] ATLAS Collaboration, Measurement of the cross-section for W boson production in association with b-jets in pp collisions at $\sqrt{s} = 7$ TeV with the ATLAS detector, JHEP 06 (2013) 084. arXiv:1302.2929, https://doi.org/10.1007/JHEP06(2013)084

[104] ATLAS Collaboration, Measurements of the Higgs boson inclusive and differential fiducial cross sections in the 4ℓ decay channel at $\sqrt{s} = 13$ TeV, Eur. Phys. J. C 80 (2020) 942. arXiv:2004.03969, https://doi.org/10.1140/epjc/s10052-020-8223-0

[105] ATLAS Collaboration, Measurements of the Higgs boson inclusive and differential fiducial cross-sections in the diphoton decay channel with pp collisions at $\sqrt{s} = 13$ TeV with the ATLAS detector, JHEP 08 (2022) 027. arXiv:2202.00487, https://doi.org/10.1007/JHEP08(2022)027

[106] M. Bähr, et al., Herwig++ physics and manual, Eur. Phys. J. C 58 (2008) 639. arXiv:0803.0883, https://doi.org/10.1140/epjc/s10052-008-0798-9

[107] J. Bellm, et al., Herwig 7.0/Herwig++ 3.0 release note, Eur. Phys. J. C 76 (4) (2016) 196. arXiv:1512.01178, https://doi.org/10.1140/epjc/s10052-016-4018-8

[108] D. de Florian, et al., LHC Higgs Cross Section Working Group, Handbook of LHC Higgs cross sections: 4. deciphering the nature of the Higgs sector (2017). 1610.07922, https://doi.org/10.23731/CYRM-2017-002

[109] A.L. Read, Presentation of search results: the CL_s technique, J. Phys. G 28 (2002) 2693, https://doi.org/10.1088/0954-3899/28/10/313

[110] ATLAS Collaboration, ATLAS Computing Acknowledgements, ATL-SOFT-PUB-2026-001, 2026. https://cds.cern.ch/record/2952666.

[111] ATLAS Collaboration, Preliminary analysis of the luminosity calibration for the ATLAS 13.6 TeV data recorded in 2023, ATL-DAPR-PUB-2024-001, 2024. https://cds.cern.ch/record/2900949.